






A microbial process for the production of benzyl acetate

Received: 24 August 2023

Accepted: 14 December 2023

Published online: 23 February 2024

 Check for updates

Kyeong Rok Choi ^{1,2}, Zi Wei Luo^{1,2}, Gi Bae Kim ¹, Hanwen Xu ¹ & Sang Yup Lee ^{1,2,3,4} 

Benzyl acetate is a valuable aromatic ester compound with diverse applications in the flavor and fragrance industries. However, its current synthesis primarily relies on inefficient plant extraction methods or chemical/enzymatic processes that depend on non-renewable substrates. Here we report a sustainable approach to benzyl acetate production from D-glucose using metabolically engineered *Escherichia coli* strains. We explored both benzoic acid-dependent and -independent synthetic pathways by either dividing the pathway between upstream and downstream strain pairs or by introducing the complete pathway into single, integrated strains. In an optimized two-phase extractive fermentation process, a delayed co-culture of an upstream strain that converts D-glucose to benzoic acid and a downstream strain that transforms benzoic acid into benzyl acetate yielded $2,238.3 \pm 171.9 \text{ mg l}^{-1}$ of benzyl acetate from D-glucose in 108 h (or $2,204.0 \pm 192.2 \text{ mg l}^{-1}$ in 96 h). The economic competitiveness of the microbial process for sustainable benzyl acetate production was also assessed by techno-economic analysis.

Benzyl acetate, an ester of benzyl alcohol and acetic acid, has a sweet and pleasant aroma reminiscent of jasmine and is extensively used as a flavor and fragrance in manufacturing foods, drinks, cosmetics, perfumes and personal hygiene/healthcare products¹. It is also used as an organic solvent for extracting plastics, resins, cellulose esters, oils and lacquers in chemical industries². Benzyl acetate is naturally synthesized as a major floral scent constituent of jasmine and ylang-ylang essential oils^{3,4}, as well as in other various flowers⁵. Yet, direct extraction of 'natural' benzyl acetate from plants is costly and insufficient to meet the global demand (as high as 10,000 metric tons per year⁶) due to its extremely low contents in the natural sources. Accordingly, benzyl acetate has been chemically synthesized through acetoxylation of toluene^{7,8} or benzylation of acetic acid⁹ using inorganic catalysts. Chemically produced benzyl acetate is labeled as an 'artificial flavor', failing to meet customers' preferences for daily commodities made with biologically produced 'natural flavors'^{10,11}.

To produce benzyl acetate using biological systems, multiple *in vitro* enzymatic processes based on transesterification of benzyl alcohol and an acyl donor (for example, vinyl acetate and ethyl acetate) have been developed using free or immobilized enzymes (mostly lipases) from diverse origins^{1,6,12–14}. In addition, *in vivo* production of $1,177.98 \pm 45.72 \text{ mg l}^{-1}$ benzyl acetate from $2,000 \text{ mg l}^{-1}$ of benzyl alcohol has been demonstrated using a recombinant *Escherichia coli* strain overexpressing the *ATF1* gene from *Saccharomyces cerevisiae* encoding an alcohol acyltransferase¹⁵. However, these bio-based processes still rely on externally supplemented substrates (that is, benzyl alcohol and/or acyl donors) that are mostly derived from petroleum.

Recently, a study reported production of $114 \pm 1 \text{ mg l}^{-1}$ of benzyl alcohol from D-glucose using a metabolically engineered *E. coli* strain harboring a synthetic pathway¹⁶. Also, multiple studies have reported *de novo* microbial production of benzoic acid^{17–19}, which can be enzymatically converted to benzyl alcohol²⁰. Briefly, a shake-flask culture

¹Metabolic and Biomolecular Engineering National Research Laboratory and Systems Metabolic Engineering and Systems Healthcare Cross-Generation Collaborative Laboratory, Department of Chemical and Biomolecular Engineering (BK21 four), Korea Advanced Institute of Science and Technology (KAIST), Daejeon, Republic of Korea. ²BioProcess Engineering Research Center, KAIST, Daejeon, Republic of Korea. ³BioInformatics Research Center, KAIST Institute for the BioCentury, and KAIST Institute for Artificial Intelligence, KAIST, Daejeon, Republic of Korea. ⁴Graduate School of Engineering Biology, KAIST, Daejeon, Republic of Korea. ✉e-mail: leesy@kaist.ac.kr

of wild-type *Streptomyces maritimus* produced 257 mg l⁻¹, 337 mg l⁻¹ and 460 mg l⁻¹ of benzoic acid from D-glucose, cellobiose and starch, respectively¹⁸, and metabolically engineered *Pseudomonas taiwanensis* harboring a β -oxidation pathway produced 232.0 mg l⁻¹ and 366.4 mg l⁻¹ of benzoic acid from D-glucose and glycerol in a shake-flask culture, respectively¹⁹. In addition, fed-batch fermentation of recombinant *E. coli* strains harboring a coenzyme A (CoA)-dependent β -oxidation route and a synthetic CoA-independent non- β -oxidation route produced 2,370 \pm 20 mg l⁻¹ and 181.0 \pm 5.8 mg l⁻¹ of benzoic acid from D-glucose, respectively, wherein the latter case co-produced 838.1 \pm 35.1 mg l⁻¹ of benzyl alcohol as an intermediate¹⁷.

In this Article, we report the development of a microbial process for benzyl acetate production from D-glucose. First, the feasibility of de novo benzyl acetate biosynthetic pathways dependent and independent of benzoic acid is demonstrated through the co-culture of upstream and downstream strain pairs (Fig. 1a,b). Next, integration of the upstream and downstream pathways into single strains is examined (Fig. 1e,f). In addition, the performances of the benzyl acetate production strains are assessed in two-phase extractive fed-batch fermentation, followed by establishment of a delayed co-culture strategy and optimization of the fermentation parameters. Finally, techno-economic analysis is conducted to analyze the economic competitiveness of the microbial process for benzyl acetate production.

Results

Benzoic acid-dependent biosynthesis

To produce benzyl acetate from D-glucose, we first designed a benzoic acid-dependent pathway based on the CoA-dependent β -oxidation route (Fig. 1a). This led to the production of 2,370 \pm 20 mg l⁻¹ benzoic acid in our recent study¹⁷. In this scheme, benzoic acid biosynthesized through the CoA-dependent β -oxidation route via L-phenylalanine is sequentially reduced to benzaldehyde and benzyl alcohol, followed by conversion into benzyl acetate. To demonstrate the feasibility of this pathway, the strategy of co-culturing an upstream strain producing benzoic acid from D-glucose and a downstream strain converting benzoic acid into benzyl acetate was implemented (Fig. 1a). In particular, the Bn1 strain harboring the CoA-dependent β -oxidation route¹⁷ was employed as the upstream strain (Fig. 2a and Supplementary Table 1). For the downstream strain, the Bn-BnAc1, Bn-BnAc2, Bn-BnAc3 and Bn-BnAc4 strains were constructed by introducing the *car* gene from *Mycobacterium marinum* (encoding a carboxylic acid reductase)²¹ and the *BEAT-2* gene from *Clarkia breweri* (encoding a variant of acetyl-CoA:benzyl alcohol acetyltransferase)²² along with either the *npt* gene from *Nocardia iowensis*²³ or the *sfp* gene from *Bacillus subtilis*²⁴ (encoding a phosphopantetheinyl transferase) into the W3110 or NST74 strains (Fig. 2a, Supplementary Table 1 and Supplementary Discussion 1), which are frequently used to produce diverse compounds or L-phenylalanine derivatives, respectively. Then, the Bn-BnAc1 and Bn-BnAc3 strains were eventually selected for the co-culture based on a benzoic acid conversion test in a shake-flask culture (Fig. 2b and Supplementary Discussions 2–4).

Co-culture of the Bn1 strain with the Bn-BnAc1 or Bn-BnAc3 strains was conducted through two-phase extractive cultivation using tributyrin as an organic phase to overcome the toxicity of benzyl acetate (Extended Data Fig. 1 and Supplementary Discussions 3 and 4). As in silico simulation suggested that the upstream/downstream biomass ratio has a substantial influence on the theoretical maximum flux of benzyl acetate biosynthesis (Fig. 1c), we examined different inoculum ratios of the Bn1 and Bn-BnAc1/Bn-BnAc3 strains (1:3, 1:1 and 3:1). As a result, production of benzyl acetate from D-glucose was observed in all co-culture conditions (Fig. 2c), demonstrating the feasibility of the benzoic acid-dependent pathway (Figs. 1a and 2a). Also, the titers ranged from about 20 mg l⁻¹ to 200 mg l⁻¹ depending on the inoculum ratio of the upstream and downstream strains used, and the highest value of 201.5 \pm 15.0 mg l⁻¹ was achieved in the co-culture of the Bn1 and Bn-BnAc3 strains with an inoculum ratio of 3:1 (Fig. 2c).

Benzoic acid-independent biosynthesis

Next, we designed an alternative pathway independent of benzoic acid based on the CoA-independent non- β -oxidation route (Fig. 1b), which enabled co-production of 181.0 \pm 5.8 mg l⁻¹ benzoic acid and 838.1 \pm 35.1 mg l⁻¹ benzyl alcohol in our recent study¹⁷ and production of 114 \pm 1 mg l⁻¹ benzyl alcohol in another study¹⁶. In this scheme, benzyl alcohol is biosynthesized via phenylpyruvic acid, an intermediate of L-phenylalanine, and further converted into benzyl acetate. To demonstrate the feasibility of this strategy, co-culture of an upstream strain producing benzyl alcohol from D-glucose and a downstream strain converting benzyl alcohol to benzyl acetate was implemented (Fig. 1b). For the upstream strain, BnOH1, BnOH2, BnOH3, BnOH4, BnOH5, BnOH6 and BnOH7 strains were constructed by overexpressing the *mdlB*, *mdlC*, *yjgB*, *aad* and mutant *hmas* genes in the LLD9 strain (derived from the NST74 strain for enhanced supply of phenylpyruvic acid) in different combinations, as described in Supplementary Discussion 5. Among the seven strains, the BnOH7 strain was selected for the co-culture based on benzyl alcohol production performance in shake-flask culture (Fig. 3a,b and Supplementary Table 1). Also, the BnOH-BnAc1 and BnOH-BnAc2 strains were constructed as downstream strains by introducing the *BEAT-2* gene from *C. breweri* (encoding a variant of acetyl-CoA:benzyl alcohol acetyltransferase) into the NST74 and LLD9 strains, respectively (Fig. 3b and Supplementary Table 1).

Two-phase extractive co-cultures of the BnOH7 and BnOH-BnAc1/BnOH-BnAc2 strains were conducted with the inoculum ratios of 1:3, 1:1 and 3:1 as well, as it was again predicted by in silico simulation that benzyl acetate biosynthesis flux was dependent on the biomass ratio of the upstream and downstream strains (Fig. 1d). Production of benzyl acetate in all co-culture conditions demonstrated the feasibility of the benzoic acid-independent pathway, and the highest benzyl acetate titer of 88.1 \pm 6.7 mg l⁻¹ was achievable when the BnOH7 and BnOH-BnAc2 strains were cultured together at the inoculum ratio of 1:1 (Fig. 3c).

Construction of integrated strains

According to the in silico simulation, introduction of the complete biosynthetic pathway into a single strain, regardless of the biosynthetic routes, was expected to achieve a higher metabolic flux towards benzyl acetate than distributing the pathway into upstream and downstream strains (Fig. 1c,d). Thus, integration of the upstream and downstream pathways into single strains was pursued (Fig. 1e,f). To overexpress heterologous enzymes for the benzoic acid-dependent pathway in a single strain (Fig. 1e), plasmid pBBR1-*car-npt-BEAT2* overexpressing the *car*, *npt* and *BEAT-2* genes from the downstream strain Bn-BnAc3 was constructed (Supplementary Table 1). This downstream plasmid and the upstream plasmids pTrcRg, pCDFL and pTacBCE from the Bn1 strain, however, could not be introduced together into a single strain even after various trials despite of the well-known compatibility of their replication origins (that is, ColE1, CloDF13, p15A and pBBR1, respectively). On the basis of this observation, the metabolic burden was suspected to be induced from unexpected interference of the upstream and downstream modules of the benzoic acid-dependent pathway.

Then, introduction of the complete benzoic acid-independent pathway into a single strain was examined (Fig. 1f). First, the heterologous genes overexpressed in the upstream and downstream strains were introduced together into the LLD9 strain (Supplementary Discussion 6), generating ten integrated strains, BnAc1–BnAc10 (Fig. 4a and Supplementary Table 1). In two-phase extractive culture, however, the BnAc1–BnAc10 strains produced less than 65 mg l⁻¹ of benzyl acetate (Fig. 4b). Next, the *xfpk* gene from *Bifidobacterium breve* encoding a photoketolase was additionally overexpressed in the BnAc1–BnAc10 strains to facilitate the supply of acetyl-CoA (an acetate donor for converting benzyl alcohol to benzyl acetate), generating another ten strains, BnAc11–BnAc20 (Fig. 4a, Supplementary Discussion 6 and Supplementary Table 1). Indeed, some of the new strains showed

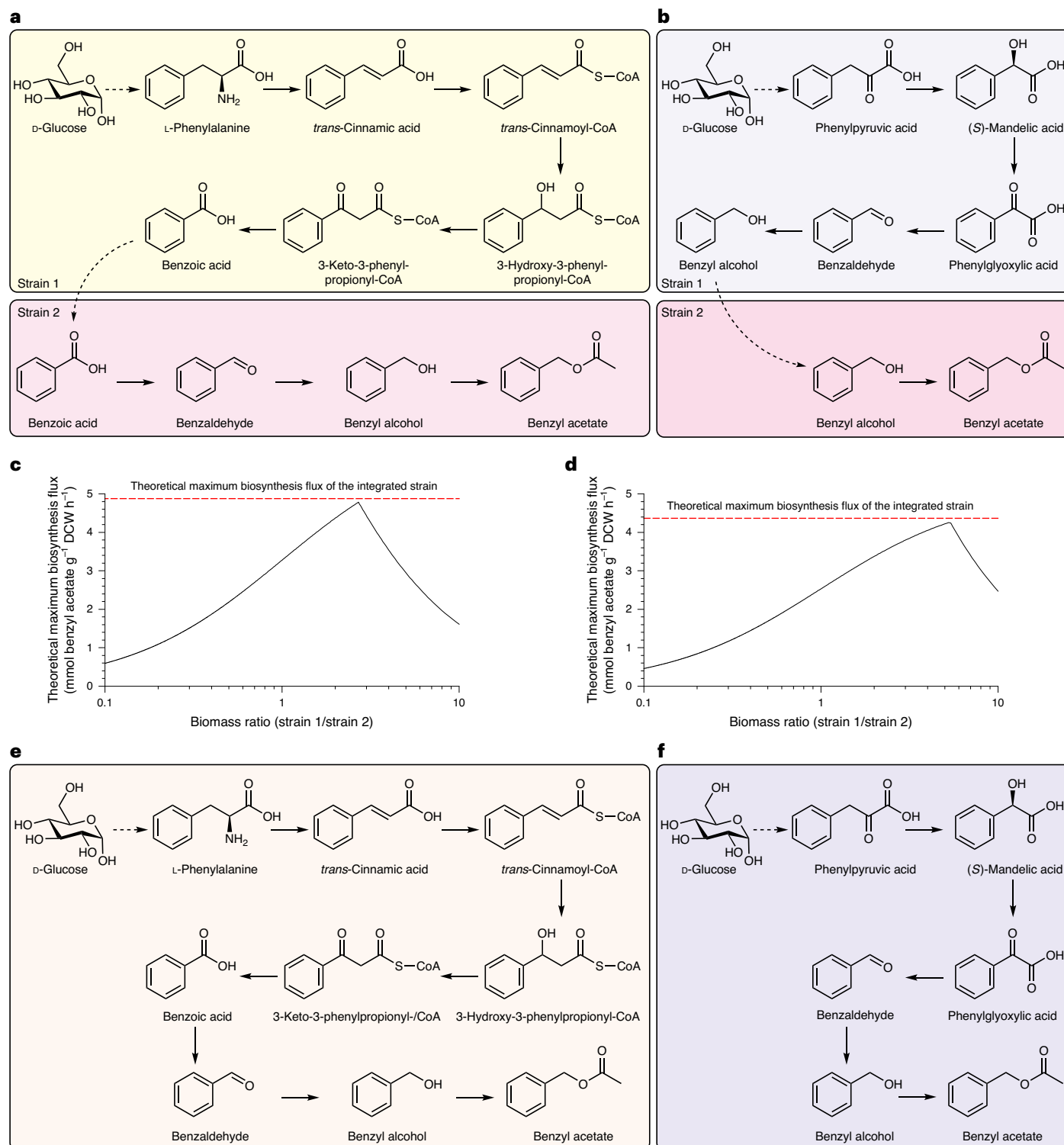


Fig. 1 | Schemes of benzoic acid-dependent and -independent pathways for de novo production of benzyl acetate from D-glucose. a, Scheme of benzoic acid-dependent pathway distributed to upstream and downstream strains for production of benzyl acetate from D-glucose through co-culture. **b**, Scheme of benzoic acid-independent pathway distributed to upstream and downstream strains for production of benzyl acetate from D-glucose through co-culture. **c**, In silico simulation of theoretical maximum biosynthesis flux of benzyl acetate through the benzoic acid-dependent pathway with respect to the

biomass ratio of the upstream and downstream strains. **d**, In silico simulation of theoretical maximum biosynthesis flux of benzyl acetate through the benzoic acid-independent pathway with respect to the biomass ratio of the upstream and downstream strains. **e**, Scheme of complete benzoic acid-dependent pathway introduced into a single strain. **f**, Scheme of complete benzoic acid-independent pathway introduced into a single strain. Strain 1, upstream strain; strain 2, downstream strain.

substantially improved benzyl acetate titers as high as $138.4 \pm 11.4 \text{ mg l}^{-1}$ (the BnAc20 strain) in two-phase extractive culture (Fig. 4c). Moreover, the *pta* gene from *Clostridium kluyveri* encoding a phosphate

acetyltransferase was additionally introduced into the BnAc11–BnAc20 strains, aiming at further enhancement of benzyl acetate production (Fig. 4a and Supplementary Discussion 6). Among the resulting

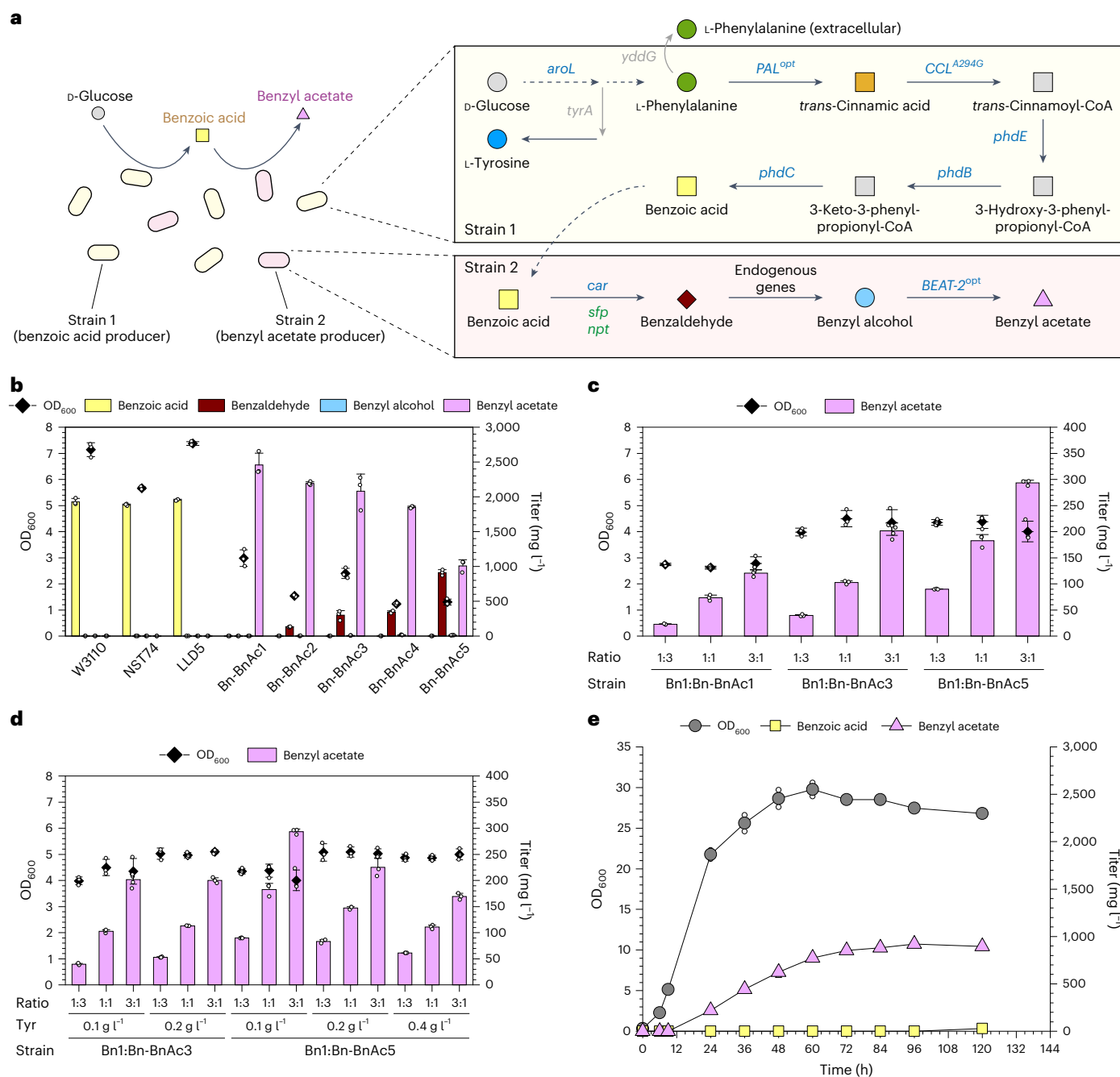


Fig. 2 | Production of benzyl acetate through co-culture of upstream and downstream strains harboring the benzoic acid-dependent pathway.

a, Scheme of producing benzyl acetate from D-glucose through co-culture of the upstream strain (strain 1) and downstream strain (strain 2) harboring the benzoic acid-dependent pathway and relevant genes. Overexpressed heterologous genes are colored blue and the genes involved in activating the carboxylic acid reductase (encoded by the *car* gene) are colored green. Knocked-out endogenous genes are colored gray. **b**, Results of benzoic acid conversion test in two-phase extractive shake-flask culture supplemented with 2 g l⁻¹ of benzoic acid ($n = 3$). **c**, Production

of benzyl acetate from D-glucose in two-phase extractive shake-flask culture by co-culture of the Bn1 strain with either of the Bn-BnAc1, Bn-BnAc3 or Bn-BnAc5 strains with a volumetric inoculum ratio of 1:3, 1:1 or 3:1 ($n = 3$). **d**, Effect of L-tyrosine (Tyr) concentration on benzyl acetate titer and cell density in two-phase extractive flask culture ($n = 3$). **e**, Production of benzyl acetate through co-culture of the Bn1 and Bn-BnAc3 strains in two-phase extractive fermentation with a volumetric inoculum ratio of 3:1 ($n = 2$). The bars and solid symbols represent mean values of biological triplicates (**b–d**) or duplicates (**e**) and smaller open symbols represent raw data points. Error bars represent standard deviations.

BnAc21–BnAc30 strains, the BnAc30 strain produced the highest level of benzyl acetate (148.9 ± 1.9 mg l⁻¹) out of the total 30 strains harboring the complete benzoic acid-independent pathway (Fig. 4b–d). This titer is much higher than the highest value (88.1 ± 6.7 mg l⁻¹) achievable in the co-culture of the BnOH7 and BnOH-BnAc2 strains (Fig. 3c), although the latter two strains do not overexpress the heterologous *xfpk* and *pta* genes.

Two-phase extractive fermentation

Two-phase extractive fed-batch fermentation was conducted with an initial volume of 2 l to assess the capacities of the three benzyl acetate production schemes constructed in this study (Figs. 2a, 3a and 4a). In duplicate rounds of fermentation, co-culture of the Bn1 and Bn-BnAc3 strains (harboring the benzoic acid-dependent pathway) with an inoculum ratio of 3:1, which led to the highest benzyl acetate

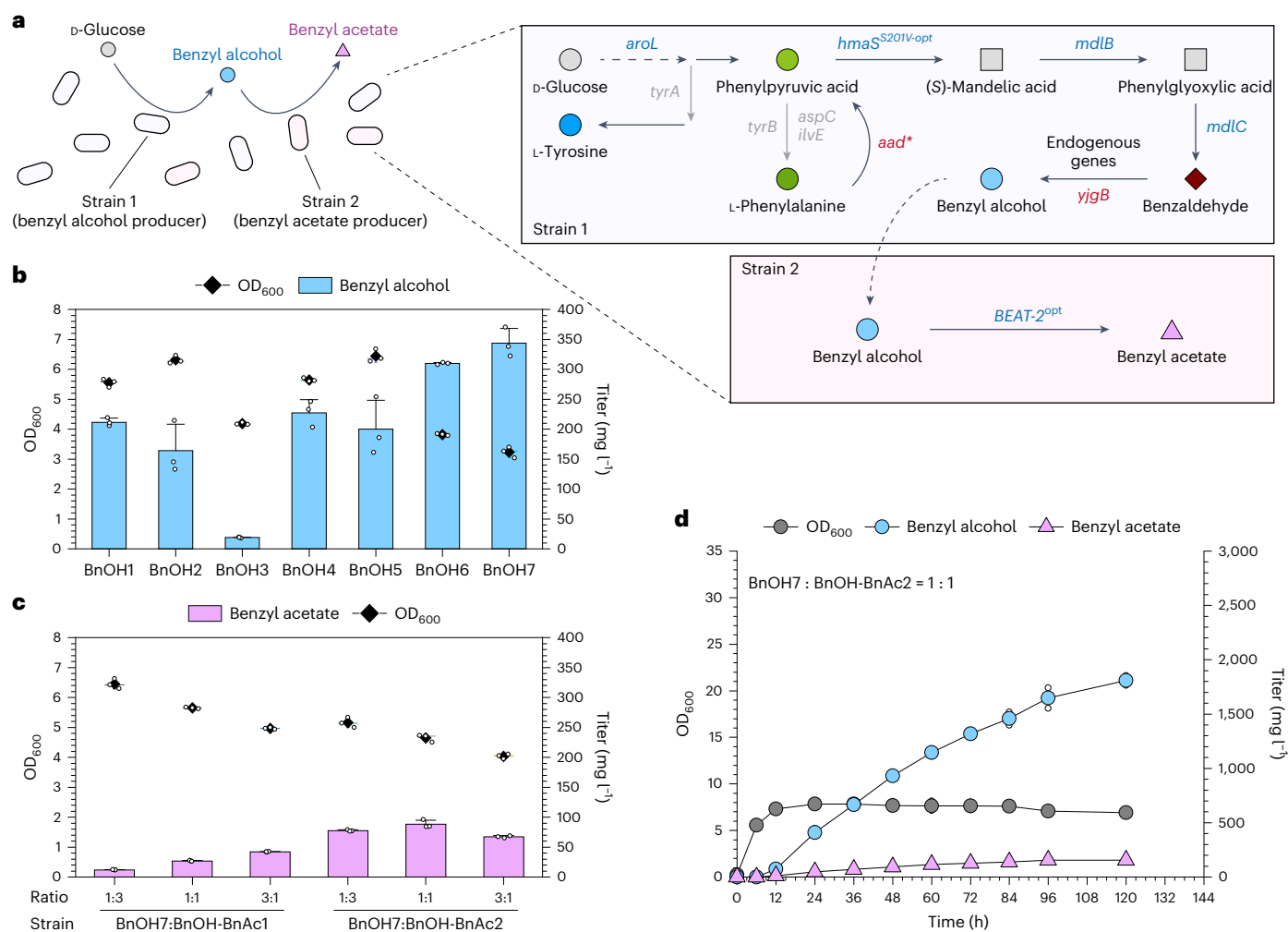


Fig. 3 | Production of benzyl acetate through co-culture of upstream and downstream strains harboring the benzoic acid-independent pathway. **a**, Scheme of producing benzyl acetate from D-glucose through co-culture of the upstream strain (strain 1) and downstream strain (strain 2) harboring the benzoic acid-independent pathway and relevant genes. Heterologous genes overexpressed only in some of the upstream strains are colored red and other heterologous genes overexpressed in the downstream strain or all of the upstream strains are colored blue (Supplementary Table 1). Knocked-out endogenous genes are labeled gray. **b**, Results of benzyl alcohol production test

in single-phase shake-flask culture (n = 3). **c**, Production of benzyl acetate from D-glucose in two-phase extractive shake-flask culture by co-culture of the BnOH7 strain with either of the BnOH-BnAc1 or BnOH-BnAc2 strain with a volumetric inoculum ratio of 1:3, 1:1 or 3:1 (n = 3). **d**, Production of benzyl acetate through co-culture of the BnOH7 and BnOH-BnAc2 strains in two-phase extractive fermentation with a volumetric inoculum ratio of 1:1 (n = 2). The bars and solid symbols represent mean values of biological triplicates (**b** and **c**) or duplicates (**d**) and smaller open symbols represent raw data points. Error bars represent standard deviations.

titer in the shake-flask culture (Fig. 2c), produced 919.3 ± 16.0 mg l⁻¹ of benzyl acetate after 96 h (Fig. 2e and Extended Data Fig. 2a,b). In contrast, co-culture of the BnOH7 and BnOH-BnAc2 strains (harboring the benzoic acid-independent pathway) with an inoculum ratio of 1:1, which led to the highest benzyl acetate titer in the shake-flask culture (Fig. 3c), produced only 154.4 ± 4.5 mg l⁻¹ of benzyl acetate after 96 h (Fig. 3d and Extended Data Fig. 2c,d). Also, $1,647.2 \pm 134.9$ mg l⁻¹ of benzyl alcohol remained unconverted by the downstream strain BnOH-BnAc2, whereas residual benzoic acid was not detected in the co-culture of the Bn1 and Bn-BnAc3 strains (Fig. 2e and Extended Data Fig. 2a,b). The highest benzyl acetate titer of $1,779.7 \pm 35.1$ mg l⁻¹ was achieved in two-phase extractive fermentation of the BnAc30 strain harboring the complete benzoic acid-independent pathway (Fig. 4e and Extended Data Fig. 2e,f). Yet, $1,181.8 \pm 48.1$ mg l⁻¹ of benzyl alcohol still remained unconverted, suggesting ineffective conversion of benzyl alcohol to benzyl acetate due to the partitioning of benzyl alcohol to the organic phase (that is, tributyrin) at a partition coefficient of 8.4 ± 0.1 (Supplementary Discussion 2).

Adjustment of biomass density and ratio

As the cell density of the BnAc30 strain in fermentation was much lower than that in the fermentation of the Bn1 and Bn-BnAc3 strains (Figs. 2e and 4e), we optimized the medium composition to increase the cell density, as an elevated cell density can contribute to improving the product titer^{25,26} (Supplementary Discussion 7). As a result, an increase in yeast extract concentration was found to increase the cell density, yet it unexpectedly decreased benzyl acetate titer (Extended Data Fig. 3). Thus, we focused on optimizing the fermentation of the Bn1 and Bn-BnAc3 strains that achieved the second highest benzyl acetate titer (Fig. 2e).

In shake-flask culture, co-culture of the Bn1 and Bn-BnAc3 strains resulted in the highest benzyl acetate titer (201.5 ± 15.0 mg l⁻¹; Fig. 2c). In two-phase extractive fermentation, however, the Bn1 and Bn-BnAc3 strains achieved lower benzyl acetate titer (919.3 ± 16.0 mg l⁻¹; Fig. 2e) than the BnAc30 strain ($1,779.7 \pm 35.1$ mg l⁻¹; Fig. 4e), probably due to the unoptimized fermentation condition. As the Bn1 strain is auxotrophic to L-tyrosine (that is, cannot synthesize L-tyrosine and hence requires

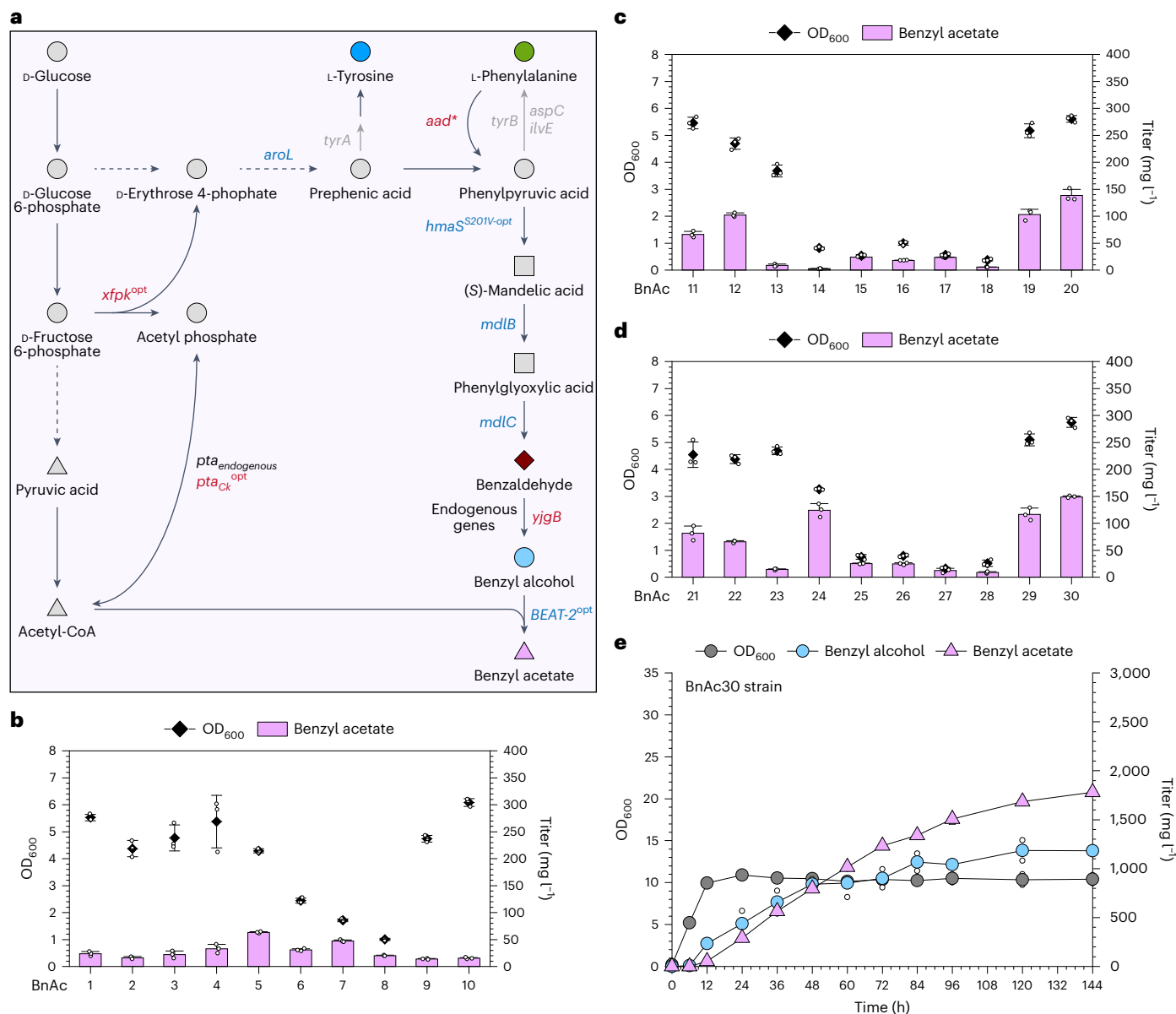


Fig. 4 | Production of benzyl acetate by the BnAc1–BnAc30 strains harboring the complete benzoic acid-independent pathway. **a**, Scheme of producing benzyl acetate from D-glucose through the complete benzoic acid-independent pathway and relevant genes. Heterologous genes overexpressed only in some of the strains are colored red and other heterologous genes overexpressed in all strains are colored blue (Supplementary Table 1). Knocked-out endogenous genes are labeled gray. **b**, Production of benzyl acetate from D-glucose in two-phase extractive shake-flask culture of the BnAc1–BnAc10 strains ($n = 3$).

c, Production of benzyl acetate from D-glucose in two-phase extractive shake-flask culture of the BnAc11–BnAc20 strains ($n = 3$). **d**, Production of benzyl acetate from D-glucose in two-phase extractive shake-flask culture of the BnAc21–BnAc30 strains ($n = 3$). **e**, Production of benzyl acetate through in two-phase extractive fermentation of the BnAc30 strain ($n = 2$). The bars and solid symbols represent mean values of biological triplicates (**b–d**) or duplicates (**e**) and smaller open symbols represent raw data points. Error bars represent standard deviations.

external supplementation of L-tyrosine to grow) due to the *tyrA* gene (involved in the L-tyrosine biosynthesis) knockout, it was thought that the prototrophic (that is, can synthesize all metabolites required for growth from a basic carbon source, such as D-glucose) Bn-BnAc3 strain outgrew the Bn1 strain during the co-culture and shifted the biomass ratio between the Bn1 and Bn-BnAc3 strains to a suboptimal point (Extended Data Fig. 4a and Supplementary Table 1). To examine this hypothesis, we examined two alternative strategies for alleviating the undesired outgrowth of the Bn-BnAc3 strain: use of an auxotrophic variant of the Bn-BnAc3 strain (that is, the Bn-BnAc5 strain; Extended Data Fig. 4b, Supplementary Discussion 8 and Supplementary Table 1) and delayed inoculation of the Bn-BnAc3 strain (Fig. 5a and Supplementary Discussion 9).

Co-culture of the Bn-BnAc5 strain derived from the auxotrophic LLD5 strain (the Bn1 strain as the parental strain; Supplementary Table 1) with the Bn1 strain resulted in improved production of benzyl acetate in fermentation ($1,460.0 \text{ mg l}^{-1}$ after 108 h; Extended Data Fig. 4c). Unexpectedly, however, $1,557.8 \text{ mg l}^{-1}$ of cinnamyl acetate was also produced from *trans*-cinnamic acid (Supplementary Discussion 8), a key intermediate of the upstream benzoic acid-dependent pathway, by promiscuous catalytic activities of the downstream enzymes (Extended Data Fig. 4d). Although cinnamyl acetate is also a valuable ester compound used as flavor and fragrance in manufacturing foods, beverages and cosmetics²⁷, more selective production of benzyl acetate, our target product, was pursued.

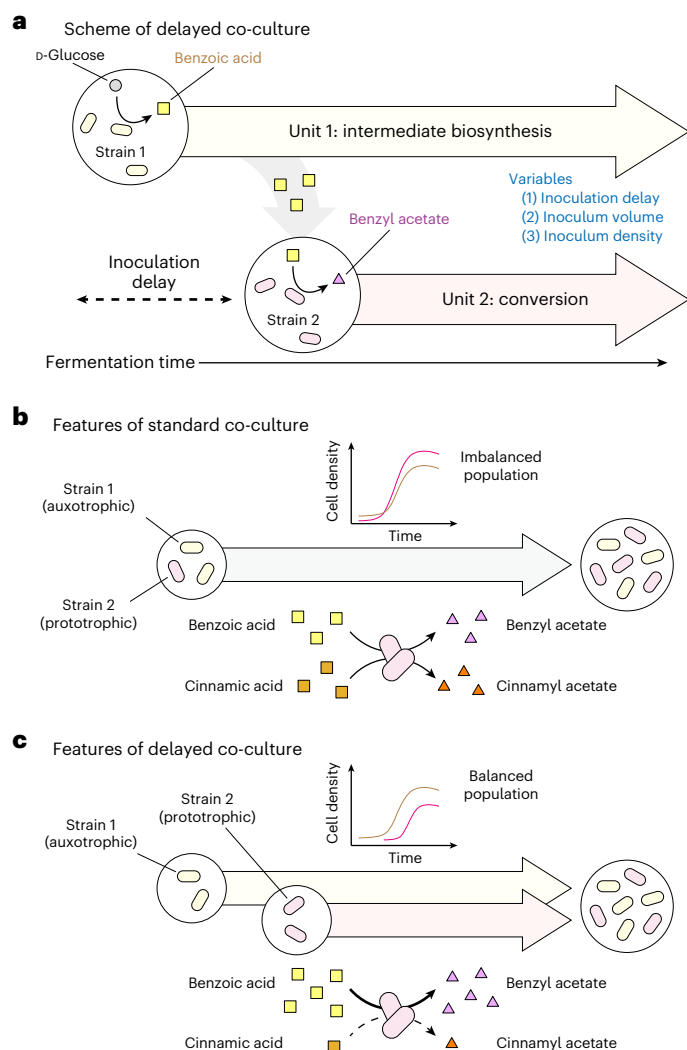
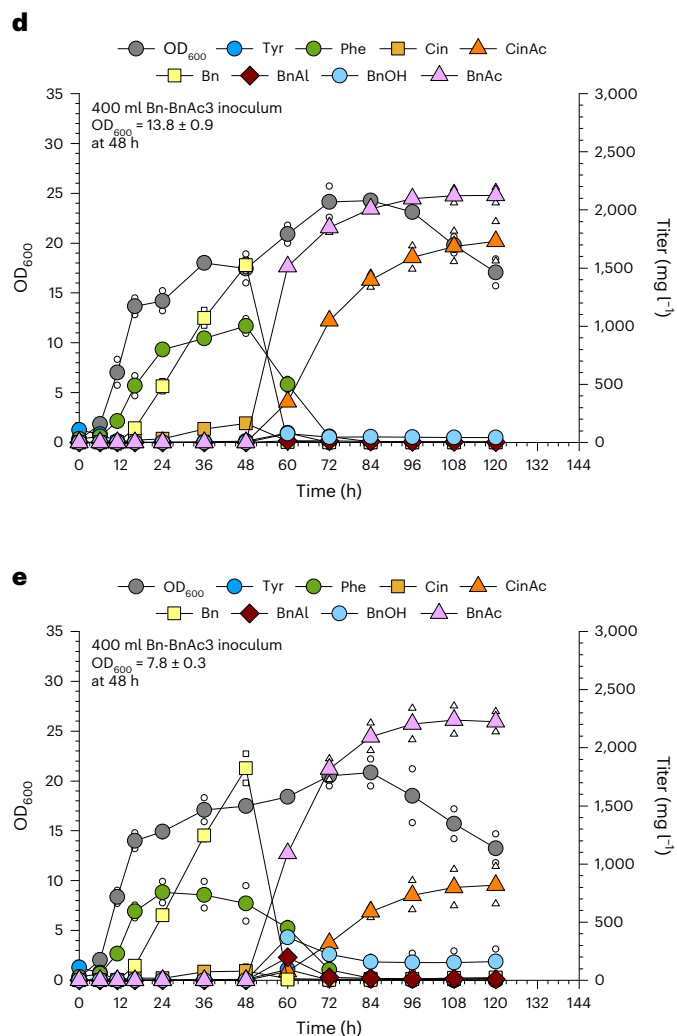


Fig. 5 | Delayed co-culture of the Bn1 and Bn-BnAc3 strains for improved production of benzyl acetate through the benzoic acid-independent pathway. **a**, Scheme of delayed co-culture for benzyl acetate production. The upstream strain (strain 1) first operates the unit process 1 responsible for producing benzoic acid (a key intermediate of the benzoic acid-dependent pathway) from D-glucose. Then, the downstream strain (strain 2) is introduced after an inoculation delay and operates the unit process 2 responsible for converting benzoic acid into benzyl acetate. The inoculation delay, inoculum volume and inoculum density are three characteristic variables modulating the delayed co-culture. **b**, In standard co-culture, the prototrophic Bn-BnAc3 strain (strain 2) outgrows the auxotrophic Bn1 strain (strain 1) and shows notable promiscuous conversion of *trans*-cinnamic acid into cinnamyl acetate. **c**, In delayed co-culture, the Bn-BnAc3 strain is introduced after enough biomass

In delayed co-culture, the outgrowth of the prototrophic Bn-BnAc3 strain in the co-culture with the auxotrophic Bn1 strain was exploited to produce a target amount of benzoic acid first (unit process 1) and then convert benzoic acid into benzyl acetate upon delayed inoculation of the Bn-BnAc3 strain (unit process 2), expecting reduced conversion of *trans*-cinnamic acid into cinnamyl acetate due to its relatively lower concentration than that of benzoic acid (Fig. 5a–c and Supplementary Discussion 9). Indeed, 1,932.6 mg l⁻¹ of benzyl acetate was produced after 108 h of fermentation along with much reduced 544.8 mg l⁻¹ of cinnamyl acetate when 200 ml of the Bn-BnAc3 strain inoculum was added at 48 h point (Extended Data Fig. 5c), demonstrating the feasibility of the delayed co-culture strategy for improving benzyl acetate titer and reducing by-product formation. It should also



of the Bn1 strain is generated to limit outgrowth of the Bn-BnAc3 strain. The prototrophic Bn-BnAc3 strain can maintain the growth even after the auxotrophic Bn1 strain reaches the stationary phase. At this point, a relatively higher concentration of benzoic acid pre-produced by the Bn1 strain helps more efficient conversion of benzoic acid into benzyl acetate by the Bn-BnAc3 strain, rather than promiscuous conversion of *trans*-cinnamic acid at lower concentration. **d,e**, Production of benzyl acetate in delayed co-culture of the Bn1 and Bn-BnAc3 strains with inoculation delay of 48 h: inoculation with 400 ml of the Bn-BnAc3 seed culture at OD₆₀₀ of 13.8 ± 0.9 (**d**) or 7.8 ± 0.3 (**e**). The solid symbols with lines represent mean values of biological duplicates (*n* = 2). Smaller open symbols represent raw data points. Bn, benzoic acid; BnAc, benzyl acetate; BnAl, benzaldehyde; BnOH, benzyl alcohol; Cin, *trans*-cinnamic acid; CinAc, cinnamyl acetate, Phe, L-phenylalanine; Tyr, L-tyrosine.

be noted that the delayed co-culture strategy can take the advantage of the conventional serial culture strategy while saving the cost of collecting cell-free medium.

Optimization of delayed co-culture

To improve the titer and selectivity of benzyl acetate production, the parameters for three characteristic variables in the delayed co-culture—namely, inoculation delay, inoculum volume and inoculum density—were optimized (Fig. 5a). When different inoculum delays ranging from 36 h to 96 h were first screened, addition of 200 ml inoculum at 48 h point resulted in the highest benzyl acetate titer of 1,932.6 mg l⁻¹ after 108 h of fermentation along with 338.5 mg l⁻¹ of unconverted benzyl alcohol (Extended Data Figs. 5 and 6, and Supplementary Discussion

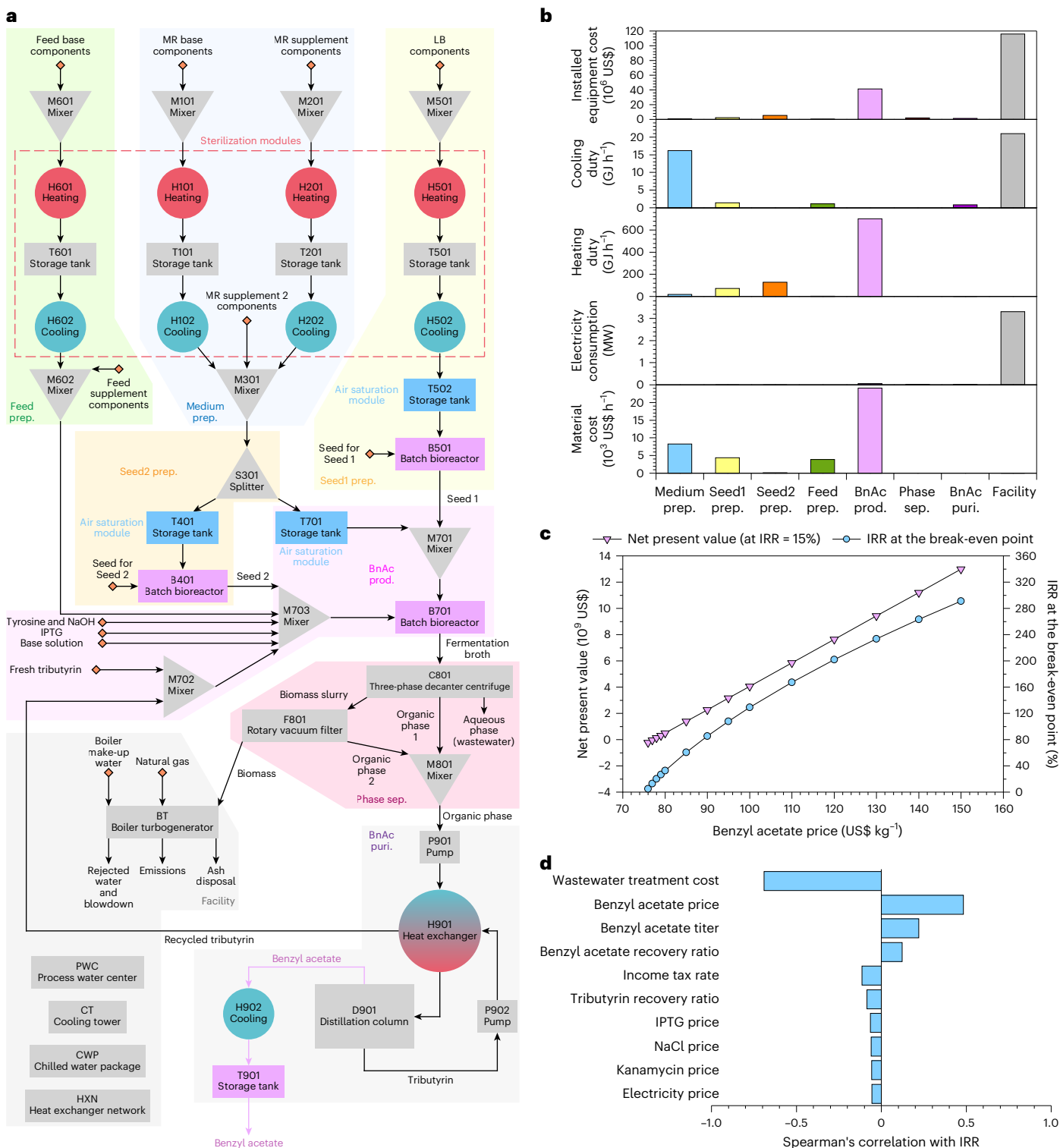


Fig. 6 | Techno-economic analysis of the microbial-based benzyl acetate production process. **a**, Overall scheme of the microbial-based benzyl acetate production designed for techno-economic analysis. The overall processes are divided into eight modules, including medium preparation (Medium prep.), seed1 preparation (Seed1 prep.), seed2 preparation (Seed2 prep.), feed preparation (Feed prep.), benzyl acetate production (BnAc prod.), phase separation (Phase sep.), benzyl acetate purification (BnAc puri.) and

infrastructural facilities (Facility). **b**, Costs of equipment, energy and material required for each module of the benzyl acetate production process. **c**, Net present value of the microbial-based benzyl acetate production business operating for 20 years with an IRR of 15.0% and the IRR values at the break-even point for a range of benzyl acetate prices. **d**, Sensitivity analysis on the IRR values at the break-even points. Examples of parameters of which perturbations have notable influence on the IRR value are presented.

10). Also, the biosynthesis rate of cinnamyl acetate in delayed co-culture was roughly proportional to that of *trans*-cinnamic acid and much lower than those of benzyl acetate, benzyl alcohol and benzaldehyde

(Extended Data Figs. 5 and 6, and Supplementary Discussion 10). In addition, the biosynthesis rates of the intermediates were the highest immediately after the delayed inoculation of the Bn-BnAc3 strain followed by

a steep decrease in the rate. Similarly, the benzyl acetate biosynthesis rate was the highest immediately after the delayed inoculation, yet the maximum value, which is much lower than those of intermediates, more gradually decreased afterwards (Extended Data Figs. 5 and 6).

Next, a doubled amount (400 ml) of the delayed inoculum was added at 48 h point to increase the conversion capacity of the second process unit and completely convert benzyl alcohol into benzyl acetate by increasing the quantity of the Bn-BnAc3 biomass (Fig. 5a and Supplementary Discussion 11). In duplicate rounds of fermentation, $2,122.4 \pm 5.0 \text{ mg l}^{-1}$ of benzyl acetate was produced at 108 h point with a notably increased benzyl acetate biosynthesis rate and a decreased residual benzyl alcohol level as low as $42.2 \pm 24.5 \text{ mg l}^{-1}$ (Fig. 5d, Extended Data Fig. 7 and Supplementary Discussion 11). However, the increased flux through the second process unit also elevated cinnamyl acetate titer to $1,685.6 \pm 184.8 \text{ mg l}^{-1}$. A similar trend with a lower benzyl acetate titer was observed when 400 ml of the delayed inoculum was added at 36 h (Extended Data Fig. 8 and Supplementary Discussion 11).

Then, lowering the cell density of the delayed inoculum (400 ml) was examined, expecting that the Bn-BnAc3 biomass at lower density immediately after the delayed inoculation would limit the promiscuous conversion of *trans*-cinnamic acid (Fig. 5c). Meanwhile, the unutilized nutrients from the 400 ml of the inoculum were expected to support the growth of the Bn-BnAc3 strain throughout the fermentation at a slower rate and contribute to effective conversion of benzyl alcohol into benzyl acetate (Supplementary Discussion 12). Indeed, reduction of the inoculum density by half (from optical density at 600 nm (OD_{600}) of 13.8 ± 0.9 to 7.8 ± 0.3) decreased cinnamyl acetate titer at 108 h to $797.8 \pm 220.9 \text{ mg l}^{-1}$ while producing $2,238.3 \pm 171.9 \text{ mg l}^{-1}$ of benzyl acetate in duplicate rounds of fermentation (Fig. 5d,e, Extended Data Figs. 9 and 10, and Supplementary Discussion 12).

Techno-economic analysis

Although the titer of benzyl acetate achieved is not yet suitable for commercial-scale production, we conducted techno-economic analysis of the process to identify factors that need improvement. On the basis of the optimized parameters and production metrics, the economic feasibility of the microbial-based benzyl acetate production through the delayed co-culture process was assessed using the BioSTEAM platform²⁸ (Supplementary Tables 2–10, Supplementary Fig. 1 and Supplementary Discussion 13). Among eight modules of the process (medium preparation, seed1 preparation, seed2 preparation, feed preparation, benzyl acetate production, phase separation, benzyl acetate purification and infrastructural facilities; Fig. 6a), the infrastructural facilities and the benzyl acetate production modules were responsible for a majority of costs for equipment, energy and material (Fig. 6b, Supplementary Tables 8 and 9, and Supplementary Fig. 2). In particular, the infrastructural facilities were calculated to require the highest cost for installing equipment (US\$116 million) as well as the highest level of cooling energy rate (21 GJ h^{-1}) and the largest consumption of electricity (3.31 MW). Also, the benzyl acetate production module was calculated to require the highest levels of heating energy rate and material cost of 703 GJ h^{-1} and $\text{US}\$24,100 \text{ h}^{-1}$, respectively (Fig. 6b, Supplementary Tables 8 and 9, and Supplementary Fig. 2).

When we assumed operation of the benzyl acetate production process for 20 years with an internal rate of return of 15.0%, the net present value became positive (US\$0.13 billion) at a benzyl acetate price of $\text{US}\$78 \text{ kg}^{-1}$ and reached $\text{US}\$4$ billion at $\text{US}\$100 \text{ kg}^{-1}$ (Fig. 6c), whereas current market prices of chemically synthesized benzyl acetate are about $\text{US}\$56\text{--}150 \text{ kg}^{-1}$ (Supplementary Tables 2 and 10). Also, the internal rate of return (IRR) value at the break-even point (that is, when the net present value is equal to zero) was estimated to be 4.8% and 129% if benzyl acetate is sold at $\text{US}\$76 \text{ kg}^{-1}$ and $\text{US}\$100 \text{ kg}^{-1}$, respectively (Fig. 6c). Moreover, sensitivity analysis revealed that the IRR value at the break-even point is most sensitive to perturbations in the

wastewater treatment cost (Fig. 6e and Supplementary Table 4). Changes in the price, titer and recovery ratio of benzyl acetate showed prominent influences as well. These results also suggest that the economic competitiveness of the process can be effectively improved by enhancing the titer and recovery efficiency of benzyl acetate as well as reducing the wastewater volume through optimization of fermentation and downstream processes, and upgrading the production strains in future studies. Finally, promiscuous formation of cinnamyl acetate and incomplete conversion of benzyl alcohol should also be addressed through further engineering of enzymes, adjustment of metabolic fluxes and optimization of fermentation process to satisfy the assumption made to perform techno-economic analysis (that is, only benzyl acetate and tributyrin exist in the organic phase; Supplementary Discussion 13).

Conclusions

In this study, we devised functional de novo biosynthetic pathways for benzyl acetate production from D-glucose. For the benzoic acid-independent pathway, the BnAc30 strain harboring the entire pathway resulted in a higher production performance ($1,779.7 \pm 35.1 \text{ mg l}^{-1}$ in 144 h; Fig. 4e) compared with co-culturing the BnOH7 and BnOH-BnAc2 strains harboring the upstream and downstream pathways, respectively ($154.4 \pm 4.5 \text{ mg l}^{-1}$ in 96 h; Fig. 3d). Co-culture of the Bn1 and Bn-BnAc3 strains harboring the upstream and downstream benzoic acid-dependent pathways, respectively, could produce $919.3 \pm 16.0 \text{ mg l}^{-1}$ benzyl acetate in 96 h (Fig. 2e), while the complete benzoic acid-dependent pathway could not be introduced into a single strain. In addition, the delayed co-culture strategy was developed to improve benzyl acetate production through co-culture of the upstream and downstream strains (Fig. 5 and Supplementary Table 14). The performance of the delayed co-culture process could be further improved through optimization of the inoculation delay, inoculum volume and inoculum density, establishing an optimized process that produce $2,238.3 \pm 171.9 \text{ mg l}^{-1}$ of benzyl acetate in 108 h (Fig. 5e). Moreover, techno-economic analysis suggested economic feasibility of the microbial-based production of benzyl acetate from D-glucose (Fig. 6c), as well as future directions towards improved economic competitiveness (Fig. 6d). The synthetic pathways and microbial strains as well as the delayed co-culture strategies and processes developed in this study potentiate replacement of the current petroleum-dependent processes for producing benzyl acetate and other valuable flavors and fragrances using more sustainable microbial processes.

Methods

Strains and media

The bacterial strains used in this study are listed in Supplementary Table 1. *E. coli* DH5 α was used for molecular cloning and plasmid propagation, while *E. coli* W3110, NST74 (ref. 29) or their derivatives were used for benzyl acetate production. For construction of plasmids and strains, *E. coli* cells were routinely cultured in the lysogeny broth (LB) medium (10 g l^{-1} tryptone, 5 g l^{-1} yeast extract and 5 g l^{-1} NaCl) or on LB-agar medium (LB medium containing 1.5% (w/v) agar). For benzyl acetate production and toxicity test, MR minimal medium containing (per liter) $6.67 \text{ g KH}_2\text{PO}_4$, $4 \text{ g (NH}_4)_2\text{HPO}_4$, $0.8 \text{ g citric acid}$, $0.8 \text{ g MgSO}_4 \cdot 7\text{H}_2\text{O}$ and $5 \text{ ml of trace metal solution}^{30}$ was used, and the pH was adjusted to 7.0 using solid NaOH. The trace metal solution (per liter) contained $10.0 \text{ g FeSO}_4 \cdot 7\text{H}_2\text{O}$, $2.65 \text{ g CaCl}_2 \cdot 2\text{H}_2\text{O}$, $2.2 \text{ g ZnSO}_4 \cdot 7\text{H}_2\text{O}$, $0.58 \text{ g MnSO}_4 \cdot 4\text{H}_2\text{O}$, $1.0 \text{ g CuSO}_4 \cdot 5\text{H}_2\text{O}$, $0.1 \text{ g (NH}_4)_6\text{Mo}_7\text{O}_{24} \cdot 4\text{H}_2\text{O}$, $0.02 \text{ g Na}_2\text{B}_4\text{O}_7 \cdot 10\text{H}_2\text{O}$ and $10 \text{ ml of fuming HCl aqueous solution}$. Stock solutions of D-glucose (500 g l^{-1}) and $\text{MgSO}_4 \cdot 7\text{H}_2\text{O}$ (80 g l^{-1}) were autoclaved separately and added to the MR medium after autoclaving the rest of the components together. Antibiotics were selectively supplemented at following concentrations when necessary: $100 \mu\text{g ml}^{-1}$ ampicillin; $50 \mu\text{g ml}^{-1}$ kanamycin; $50 \mu\text{g ml}^{-1}$ streptomycin; $34 \mu\text{g ml}^{-1}$ chloramphenicol.

Plasmid construction

Plasmids used in this study are listed in Supplementary Table 1. Oligonucleotide primers and template DNAs used for plasmid construction are listed in Supplementary Table 11 along with the construction schemes. The DNA sequences of the codon-optimized genes are listed in Supplementary Table 12. All DNA manipulations for plasmid construction were conducted according to the standard protocols³¹. The sequence of all constructed plasmids was verified by DNA sequencing.

Chromosomal gene knockout

The chromosomal *ilvE* gene was knocked out from the *E. coli* LLD6 strain¹⁷ to construct the LLD9 strain through the one-step homologous recombination protocol^{32,33} using a DNA fragment *ilvE*-KO-100 (Supplementary Table 13) and plasmids pKD46 and pJW168 (Supplementary Table 1).

Benzyl acetate toxicity test

To examine the inhibitory effect of benzyl acetate to *E. coli*, the wild-type *E. coli* W3110 strain was firstly inoculated to a test tube containing 5 ml LB medium and incubated at 37 °C and 200 rpm for 12 h. Next, 1 ml of the preculture was transferred to a 300-ml baffled flask containing 50 ml MR medium supplemented with 10 g l⁻¹ glucose and 0–1 g l⁻¹ benzyl acetate and cultured at 37 °C and 200 rpm. The inhibitory effect was evaluated by monitoring the cell growth based on the optical density at the wavelength of 600 nm (OD₆₀₀).

Partition coefficient measurement

To determine the partition coefficients of benzyl acetate and benzyl alcohol between the aqueous and organic phases, benzyl acetate and benzyl alcohol were first dissolved in MR medium without glucose at 1 g l⁻¹, and 800 μl of the resulting solutions were mixed with the equal volume of tributyrin (97 % (w/w), Thermo Scientific) in a 2-ml microcentrifuge tube. The mixtures were vortexed for 1 min and horizontally shaken at 200 rpm and 30 °C for 24 h. Subsequently, the mixtures were centrifuged at 16,000g for 20 min to separate the aqueous and organic phases, and the concentrations of benzyl acetate and benzyl alcohol in each phase were measured using high-performance liquid chromatography (HPLC) as described in 'Analytical procedures' below. Lastly, the partition coefficients were calculated by dividing the concentration in the organic phase by that in the aqueous phase.

Shake-flask culture conditions

Shake-flask cultures were conducted using the MR medium in 300-ml baffled flasks. Briefly, the precultures were prepared by inoculating test tubes containing 5 ml LB medium and incubating at 37 °C and 200 rpm for 12 h. Then, 1 ml of the precultures were transferred to baffled flasks containing 50 ml or 25 ml MR medium with 10 g l⁻¹ glucose for single-phase benzyl alcohol production or two-phase benzyl acetate production, respectively, unless mentioned otherwise. For co-culture of the upstream and downstream strains, the 1 ml of inoculum was formulated by mixing the precultures of each strain according to the indicated volumetric ratio. For example, 0.75 ml of the upstream strain preculture and 0.25 ml of the downstream preculture were mixed to generate 1 ml inoculum with the upstream and downstream inoculum ratio of 3:1. The inoculated flasks were cultured in a shaking incubator at 30 °C and 200 rpm for 60 h. At 6 h when the OD₆₀₀ reached 0.6–0.8, overexpression of the introduced genes was induced by supplementing 0.5 mM isopropyl β-D-1-thiogalactopyranoside (IPTG). For benzyl acetate production through two-phase extractive culture, 5 ml of tributyrin was also added as an organic phase to 25 ml of the culture volume at this point (that is aqueous-to-organic phase volumetric ratio of 5:1). For benzoic acid conversion test, 1 ml of 59 g l⁻¹ sodium benzoate was added to the two-phase culture broth composed of 25 ml of aqueous phase and 5 ml of organic phase (equivalent to the final benzoic acid concentration of 1.92 g l⁻¹ in the aqueous phase) at 12 h. To overcome the

auxotrophy generated by knocking out relevant genes, the following supplements were additionally supplied at the beginning of the flask culture unless indicated otherwise: 0.1 g l⁻¹ L-tyrosine and 10 mg l⁻¹ thiamine for the *tyrA* knockout; 3 g l⁻¹ L-aspartic acid for the *tyrB* and *aspC* knockouts; 0.04 mg l⁻¹ L-phenylalanine and 3 g l⁻¹ yeast extract for the *ilvE* knockout.

Fed-batch fermentation conditions

Two-phase extractive fed-batch fermentations were conducted at 30 °C using a 6.6-l fermentor (Bioflo 320; New Brunswick Scientific) containing 2 l of MR medium supplemented with 20 g l⁻¹ of glucose. Briefly, the seed culture was prepared by inoculating a test tube containing 5 ml of LB medium and incubating at 37 °C and 200 rpm for 12 h. Next, each of two 300-ml Erlenmeyer flasks containing 100 ml of LB medium were inoculated with 2 ml of the seed culture and then incubated at 37 °C and 200 rpm for 12 h. The resulting 200 ml of the preculture was transferred into the fermentor containing 1.8 l of medium containing components equivalent to 2 l of MR medium supplemented with 20 g l⁻¹ glucose. For standard co-culture of the upstream and downstream strains, the 200 ml of inoculum was formulated by mixing the precultures of each strain according to the indicated volumetric ratio. For example, 150 ml of the upstream strain preculture and 50 ml of the downstream preculture were mixed to generate 200 ml inoculum with the upstream and downstream inoculum ratio of 3:1.

During fermentation, the pH was controlled at 7.0 using saturated ammonia solution (~28%, w/w). The dissolved oxygen level was maintained at 40% of the air saturation by controlling the agitation speed within a range of 200–1,000 rpm and constantly supplying filtered air at 2.0 l min⁻¹. Once the OD₆₀₀ value reached 5 or more, 1 mM IPTG was supplemented to induce the expression of benzyl acetate biosynthesis genes and 0.4 l of tributyrin was supplied at 1.11 ml min⁻¹. Antifoam 204 (Sigma-Aldrich) was used to repress the formation of foam during fermentation. After the initial glucose was depleted, a nutrient solution was supplied at 9.4 ml min⁻¹ whenever pH value was above 7.02.

For benzyl acetate production through the benzoic acid-dependent pathway, 0.1 g l⁻¹ L-tyrosine and 10 mg l⁻¹ thiamine were supplemented to the fermentation media at the beginning, and 0.1 g l⁻¹ L-tyrosine (in forms of powder or 50 g l⁻¹ stock solution) was further supplemented at 24 h and 48 h points of the fermentation. The nutrient solution consisted of 700 g l⁻¹ glucose, 8 g l⁻¹ MgSO₄·7H₂O, 5 ml l⁻¹ trace metal solution, 10 mg l⁻¹ thiamine and 1 mM IPTG.

For benzyl acetate production through the benzoic acid-independent pathway, 0.1 g l⁻¹ L-tyrosine, 0.1 g l⁻¹ L-phenylalanine, 3 g l⁻¹ L-aspartic acid, 3 g l⁻¹ yeast extract and 10 mg l⁻¹ thiamine were supplemented to the fermentation media at the beginning. The nutrient solution contained 700 g l⁻¹ glucose, 8 g l⁻¹ MgSO₄·7H₂O, 3 g l⁻¹ yeast extract, 5 ml l⁻¹ trace metal solution, 10 mg l⁻¹ thiamine and 1 mM IPTG.

Delayed co-culture conditions

For delayed co-culture of the Bn1 and Bn-BnAc3 strains, the preculture of the Bn1 strain was prepared and transferred to a fermentor supplemented with 0.1 g l⁻¹ L-tyrosine and 10 mg l⁻¹ thiamine following the fed-batch fermentation procedures described above. Once the OD₆₀₀ value reached 5 or more, however, only 1 mM IPTG was supplemented to induce the expression of benzyl acetate biosynthesis genes without supplying tributyrin. Meanwhile, the delayed inoculum of the Bn-BnAc3 strain was prepared by inoculating each of four or eight 300-ml baffled flasks that contain 50 ml of the MR medium supplemented with 20 g l⁻¹ glucose, 0.1 g l⁻¹ L-tyrosine and 10 mg l⁻¹ thiamine with 1 ml of the Bn-BnAc3 strain seed culture (prepared as aforementioned) and culturing at 30 °C and 200 rpm for 12–15 h, depending on target cell density. Subsequently, 200 ml or 400 ml of the preculture was transferred to the fermentor at 48 h point (unless mentioned otherwise), followed by supply of 0.44 l or 0.48 l of tributyrin at 1.11 ml min⁻¹, respectively.

The rest of the conditions followed those of standard fed-batch fermentation for producing benzyl acetate through the benzoic acid-dependent pathway. Briefly, the pH was controlled at 7.0 using saturated ammonia solution (~28%, w/w). The dissolved oxygen level was maintained at 40% of the air saturation by controlling the agitation speed within a range of 200–1,000 rpm and constantly supplying filtered air at 2.0 l min⁻¹. Antifoam 204 (Sigma-Aldrich) was used to repress the formation of foam during fermentation, and 0.1 g l⁻¹ tyrosine (in forms of powder or 50 g l⁻¹ stock solution) was further supplemented at the 24 h and 48 h points of the fermentation. After the initial glucose was depleted, a nutrient solution (700 g l⁻¹ glucose, 8 g l⁻¹ MgSO₄·7H₂O, 5 ml l⁻¹ trace metal solution, 10 mg l⁻¹ of thiamine and 1 mM IPTG) was supplied at 9.4 ml min⁻¹ whenever pH value was above 7.02.

Analytical procedures

Cell density was monitored by measuring OD₆₀₀ using an Ultrospec 3100 spectrophotometer (Amersham Biosciences).

The levels of residual D-glucose, organic acids, benzyl acetate and related metabolites (for example, intermediates) were analyzed using HPLC systems. To prepare samples for HPLC analysis, culture samples were first centrifuged at 16,000g for 20 min to separate the aqueous and organic phases. The aqueous phase samples were appropriately diluted with deionized water and filtered using 0.22-μm PVDF filters, and the organic phase samples were appropriately diluted with tributyrin and filtered using 0.22-μm PTFE filters. The residual D-glucose and organic acid levels during the two-phase fed-batch fermentations were analyzed using a HPLC system operated by the Breeze2 (Database version 6.20.00.00) software and equipped with a 1515 isocratic pump and 2414 refractive index detector (Waters). A MetaCarb 87H column (7.8 × 300 mm, Agilent) was eluted isocratically with 0.01 M H₂SO₄ at 35 °C at a flow rate of 0.5 ml min⁻¹.

The concentrations of pathway metabolites were analyzed using 1260 Infinity II liquid chromatography system (Agilent) operated by the OpenLAB CDS (ChemStation Edition; version information unavailable) software and equipped with a diode array detector, monitoring absorbance at 210 nm (for L-phenylalanine, benzyl alcohol and benzyl acetate), 230 nm (for L-tyrosine, benzoic acid and cinnamyl acetate) and 255 nm (for benzaldehyde and *trans*-cinnamic acid). Poroshell 120 column (4.6 × 150 mm, Agilent) was eluted using mixed solutions of 0.1% (v/v) trifluoroacetic acid aqueous solution (buffer A) and pure acetonitrile (buffer B) flowing at 0.625 ml min⁻¹. The ratio of the buffers A and B were controlled according to the following program: 0–1 min, 90:10; 1–10 min, a linear gradient from 90:10 to 30:70; 10–12 min, 30:70; 12–14 min, a linear gradient from 30:70 to 90:10; 14–18 min, 90:10.

The overall product titers of the two-phase cultures were calculated with respect to the aqueous phase volume. Benzyl acetate, benzyl alcohol, benzaldehyde and cinnamyl acetate were mostly detected in the organic phase samples and the other metabolites were mostly detected in the aqueous phase samples. Nevertheless, we calculated the overall titers of the metabolites by dividing their concentrations in the organic phase sample by five (that is, the ratio of the aqueous phase volume to the organic phase volume) and adding to their concentrations in the aqueous phase sample.

Calculation of the theoretical maximum flux of benzyl acetate biosynthesis

Theoretical maximum fluxes of benzyl acetate biosynthesis through the benzoic acid-dependent and -independent pathways were analyzed using iML1515, a genome-scale metabolic model of *E. coli*³⁴. Each biosynthetic pathway was added to the model by introducing the following reactions. For the upstream strain (strain 1) harboring the benzoic acid-dependent pathway, the following reactions were introduced: 'L-phenylalanine → *trans*-cinnamic acid + NH₄', '*trans*-cinnamic acid + ATP + CoA → cinnamoyl-CoA + AMP + pyrophosphate', 'cinnamoyl-CoA + H₂O → 3-hydroxyphenylpropionyl-CoA',

'3-hydroxyphenylpropionyl-CoA + NAD⁺ → 3-ketophenylpropionyl-CoA + NADH + H⁺', '3-ketophenylpropionyl-CoA + H₂O → benzoic acid + acetyl-CoA + H⁺', transportation of benzoic acid to extracellular space and a benzoic acid exchange reaction. Also, the following reactions were introduced for the downstream strain (strain 2): a benzoic acid exchange reaction, transportation of benzoic acid to extracellular space, 'benzoic acid + ATP + NADPH + H⁺ → benzaldehyde + AMP + pyrophosphate + NADP⁺', 'benzaldehyde + NADPH + H⁺ → benzyl alcohol + NADP⁺', 'acetyl-CoA + benzyl alcohol → CoA + benzyl acetate', transportation of benzyl acetate to extracellular space and a benzyl acetate exchange reaction.

For the upstream strain (strain 1) harboring the benzoic acid-independent pathway, the following reactions were introduced: 'phenylpyruvic acid + O₂ → S-mandelic acid + CO₂', 'S-mandelic acid + FMN → phenylglyoxylic acid + FMNH₂', 'phenylglyoxylic acid + H⁺ → benzaldehyde + CO₂', 'benzaldehyde + NADPH + H⁺ → benzyl alcohol + NADP⁺', transportation of benzyl alcohol to extracellular space and a benzyl alcohol exchange reaction. Also, following the reactions were introduced for the downstream strain (strain 2): a benzyl alcohol exchange reaction, transportation of benzyl alcohol to extracellular space, 'acetyl-CoA + benzyl alcohol → CoA + benzyl acetate', transportation of benzyl acetate to extracellular space and a benzyl acetate exchange reaction.

For the integrated strain harboring the entire benzoic acid-dependent pathway, the following reactions were added: 'L-phenylalanine → *trans*-cinnamic acid + NH₄', '*trans*-cinnamic acid + ATP + CoA → cinnamoyl-CoA + AMP + pyrophosphate', 'cinnamoyl-CoA + H₂O → 3-hydroxyphenylpropionyl-CoA', '3-hydroxyphenylpropionyl-CoA + NAD⁺ → 3-ketophenylpropionyl-CoA + NADH + H⁺', '3-ketophenylpropionyl-CoA + H₂O → benzoic acid + acetyl-CoA + H⁺', 'benzoic acid + ATP + NADPH + H⁺ → benzaldehyde + AMP + pyrophosphate + NADP⁺', 'benzaldehyde + NADPH + H⁺ → benzyl alcohol + NADP⁺', 'acetyl-CoA + benzyl alcohol → CoA + benzyl acetate', transportation of benzyl acetate to extracellular space and a benzyl acetate exchange reaction.

Finally, for the integrated strain harboring the entire benzoic acid-independent pathway, the following reactions were added: 'phenylpyruvic acid + O₂ → S-mandelic acid + CO₂', 'S-mandelic acid + FMN → phenylglyoxylic acid + FMNH₂', 'phenylglyoxylic acid + H⁺ → benzaldehyde + CO₂', 'benzaldehyde + NADPH + H⁺ → benzyl alcohol + NADP⁺', 'acetyl-CoA + benzyl alcohol → CoA + benzyl acetate', transportation of benzyl acetate to extracellular space and a benzyl acetate exchange reaction.

To calculate the theoretical maximum flux of benzyl acetate biosynthesis in the integrated strains, flux balance analysis was conducted by maximizing the flux of benzyl acetate production reaction. To calculate the theoretical maximum flux of benzyl acetate biosynthesis in the co-culture systems, we constructed a combined model of strain 1 and strain 2 (that is, upstream and downstream strains, respectively) whose components are separated by their own compartments. We solved the following optimization problem for the combined model:

$$\max v_{\text{benzylacetateproduction}}$$

$$\text{s.t. } \sum_{j \in M} S_{i,j}^k v_j^k = 0, \forall i \in N^k$$

$$v_{j,lb}^k \leq v_j^k \leq v_{j,ub}^k, \forall j \in M^k$$

$$\chi^1 v_{\text{inter}}^1 + \chi^2 v_{\text{inter}}^2 \geq 0$$

In the above optimization problem, the variables are defined as follows: v_j^k , a flux of a metabolic reaction j in strain k ; $S_{i,j}^k$, a coefficient of metabolite i which participates in metabolic reaction j in strain k ;

$v_{j,ub}^k$, the upper bound of a metabolic reaction j in strain k ; $v_{j,lb}^k$, the lower bound of a metabolic reaction j in strain k ; v_{inter}^k , a flux of the intermediate chemical (that is, benzoic acid for benzoic acid-dependent pathway and benzyl alcohol for benzoic acid-independent pathway) production of strain k ; X^k , the cell density of strain k ; N^k and M^k represent the sets of metabolites and reactions of strain k , respectively. s.t., such that. We assumed no biomass production or ATP requirement for non-growth associated maintenance when calculating the theoretical maximum flux of benzyl acetate biosynthesis. Thus, the specific cell growth rate was set to zero, leading to constant cell densities. Therefore, the above optimization problem can be formulated as follows, where $n = X^2/X^1$.

$$\max v_{\text{benzylacetate production}}$$

$$\text{s.t. } \sum_{j \in M} S_{i,j}^k v_j^k = 0, \forall i \in N^k$$

$$v_{j,lb}^k \leq v_j^k \leq v_{j,ub}^k, \forall j \in M^k$$

$$v_{inter}^1 + n v_{inter}^2 \geq 0$$

To analyze the theoretical maximum flux of benzyl acetate production of the co-culture system based on the ratio of cell density between strain 1 and strain 2 (that is, the upstream and downstream strains), the optimization problem was solved with varying n . Throughout the simulations, the upper bound of glucose uptake flux was set at 10 mmol g⁻¹ dry cell weight (DCW) h⁻¹ and the ATP maintenance requirement was set at 0 mmol g⁻¹ DCW h⁻¹.

Techno-economic analysis and sensitivity analysis

A microbial fermentation-based configuration for production of benzyl acetate from D-glucose was developed in BioSTEAM (Fig. 6a and Supplementary Discussion 13). Techno-economic analysis of the microbial-based benzyl acetate production process based on the delayed co-culture of the Bn1 and Bn-BnAc3 strains and sensitivity analysis on the internal rate of return at the break-even point were conducted based on the configuration constructed in BioSTEAM and a set of parameters surveyed from diverse sources (Supplementary Tables 2–4). Supplementary Discussion 13 provides a detailed information on the techno-economic analysis and the sensitivity analysis conducted in this study.

Reporting summary

Further information on research design is available in the Nature Portfolio Reporting Summary linked to this article.

Data availability

All source data for figures have been deposited at figshare (<https://doi.org/10.6084/m9.figshare.24026634>).

Code availability

All codes used for calculating the theoretical maximum flux of benzyl acetate biosynthesis and techno-economic analysis of the microbial-based benzyl acetate production are available at <https://github.com/kaistsystemsbiology/BenzylAcetateFluxAnalysis> and <https://github.com/kaistsystemsbiology/BenzylAcetateTEA>.

References

- Majumder, A. B., Singh, B., Dutta, D., Sadhukhan, S. & Gupta, M. N. Lipase catalyzed synthesis of benzyl acetate in solvent-free medium using vinyl acetate as acyl donor. *Bioorg. Med. Chem. Lett.* **16**, 4041–4044 (2006).
- Radnik, J. et al. Deactivation of Pd acetoxylation catalysts: direct observations by XPS investigations. *Angew. Chem. Int. Ed.* **44**, 6771–6774 (2005).
- Ahmed, N., Hanani, Y. A., Ansari, S. Y. & Anwar, S. in *Essential Oils in Food Preservation, Flavor and Safety* (ed Preedy, V. R.) 487–494 (Elsevier, 2016).
- Mallavarapu, G., Gurudutt, K. & Syamasundar, K. in *Essential Oils in Food Preservation, Flavor and Safety* (ed Preedy, V. R.) 865–873 (Elsevier, 2016).
- Knudsen, J. T., Tollsten, L. & Bergström, L. G. Floral scents—a checklist of volatile compounds isolated by head-space techniques. *Phytochemistry* **33**, 253–280 (1993).
- Garlapati, V. K., Kumari, A., Mahapatra, P. & Banerjee, R. Modeling, simulation, and kinetic studies of solvent-free biosynthesis of benzyl acetate. *J. Chem.* **2013**, 451652 (2013).
- Benhmid, A., Narayana, K. V., Martin, A. & Lucke, B. One-step synthesis of benzyl acetate by gas phase acetoxylation of toluene over highly active and selective Pd-Sb-TiO₂ catalysts. *Chem. Commun.* <https://doi.org/10.1039/b406396a> (2004).
- Komatsu, T., Inaba, K., Uezono, T., Onda, A. & Yashima, T. Nano-size particles of palladium intermetallic compounds as catalysts for oxidative acetoxylation. *Appl. Catal. A* **251**, 315–326 (2003).
- Nandiwale, K. Y., Galande, N. D., Raut, S. A. & Bokade, V. V. Benzylolation of acetic acid to benzyl acetate over highly active and reusable micro/meso-HZSM-5. *Chem. Eng. Res. Des.* **93**, 584–590 (2015).
- Park, Y. C., Shaffer, C. E. & Bennett, G. N. Microbial formation of esters. *Appl. Microbiol. Biotechnol.* **85**, 13–25 (2009).
- Luo, Z. W., Cho, J. S. & Lee, S. Y. Microbial production of methyl anthranilate, a grape flavor compound. *Proc. Natl Acad. Sci. USA* **116**, 10749–10756 (2019).
- Perdomo, I. C. et al. Efficient enzymatic preparation of flavor esters in water. *J. Agric. Food Chem.* **67**, 6517–6522 (2019).
- Melo, A. D. Q. et al. Synthesis of benzyl acetate catalyzed by lipase immobilized in nontoxic chitosan-polyphosphate beads. *Molecules* <https://doi.org/10.3390/molecules22122165> (2017).
- Gómez, J. et al. Biosynthesis of benzyl acetate: optimization of experimental conditions, kinetic modelling and application of alternative methods for parameters determination. *Bioresour. Technol. Rep.* **11**, 100519 (2020).
- Lee, J. W. & Trinh, C. T. Microbial biosynthesis of lactate esters. *Biotechnol. Biofuels* **12**, 226 (2019).
- Pugh, S., McKenna, R., Halloum, I. & Nielsen, D. R. Engineering *Escherichia coli* for renewable benzyl alcohol production. *Metab. Eng. Commun.* **2**, 39–45 (2015).
- Luo, Z. W. & Lee, S. Y. Metabolic engineering of *Escherichia coli* for the production of benzoic acid from glucose. *Metab. Eng.* **62**, 298–311 (2020).
- Noda, S., Kitazono, E., Tanaka, T., Ogino, C. & Kondo, A. Benzoic acid fermentation from starch and cellulose via a plant-like beta-oxidation pathway in *Streptomyces maritimus*. *Microb. Cell Fact.* **11**, 49 (2012).
- Otto, M., Wynands, B., Marienhagen, J., Blank, L. M. & Wierckx, N. Benzoate synthesis from glucose or glycerol using engineered *Pseudomonas taiwanensis*. *Biotechnol. J.* **15**, e2000211 (2020).
- Venkatasubramanian, P., Daniels, L., Das, S., Lamm, A. S. & Rosazza, J. P. Aldehyde oxidoreductase as a biocatalyst: reductions of vanillic acid. *Enzyme Microb. Technol.* **42**, 130–137 (2008).
- Akhtar, M. K., Turner, N. J. & Jones, P. R. Carboxylic acid reductase is a versatile enzyme for the conversion of fatty acids into fuels and chemical commodities. *Proc. Natl Acad. Sci. USA* **110**, 87–92 (2013).
- Dudareva, N., D'Auria, J. C., Nam, K. H., Raguso, R. A. & Pichersky, E. Acetyl-CoA:benzylalcohol acetyltransferase—an enzyme involved in floral scent production in *Clarkia breweri*. *Plant J* **14**, 297–304 (1998).

23. Venkitasubramanian, P., Daniels, L. & Rosazza, J. P. Reduction of carboxylic acids by *Nocardia* aldehyde oxidoreductase requires a phosphopantetheinylated enzyme. *J. Biol. Chem.* **282**, 478–485 (2007).
24. Quadri, L. E. et al. Characterization of Sfp, a *Bacillus subtilis* phosphopantetheinyl transferase for peptidyl carrier protein domains in peptide synthetases. *Biochemistry* **37**, 1585–1595 (1998).
25. Choi, K. R., Yu, H. E., Lee, H. & Lee, S. Y. Improved production of heme using metabolically engineered *Escherichia coli*. *Biotechnol. Bioeng.* **119**, 3178–3193 (2022).
26. Choi, K. R., Yu, H. E. & Lee, S. Y. Production of zinc protoporphyrin IX by metabolically engineered *Escherichia coli*. *Biotechnol. Bioeng.* **119**, 3319–3325 (2022).
27. Bhatia, S. P. et al. Fragrance material review on cinnamyl acetate. *Food Chem. Toxicol.* **45**, S53–S57 (2007).
28. Cortes-Pena, Y., Kumar, D., Singh, V. & Guest, J. S. BioSTEAM: a fast and flexible platform for the design, simulation, and techno-economic analysis of biorefineries under uncertainty. *ACS Sustain. Chem. Eng.* **8**, 3302–3310 (2020).
29. Tribe, D. E. Novel microorganism and method. US patent 4,681,852 (1987).
30. Lee, Y. & Lee, S. Y. Enhanced production of poly (3-hydroxybutyrate) by filamentation-suppressed recombinant *Escherichia coli* in a defined medium. *J. Environ. Polym. Degrad.* **4**, 131–134 (1996).
31. Sambrook, J. & Russell, D. W. *Molecular Cloning: A Laboratory Manual* (Cold Spring Harbor Laboratory, 2001).
32. Datsenko, K. A. & Wanner, B. L. One-step inactivation of chromosomal genes in *Escherichia coli* K-12 using PCR products. *Proc. Natl Acad. Sci. USA* **97**, 6640–6645 (2000).
33. Zhao, X. R., Choi, K. R. & Lee, S. Y. Metabolic engineering of *Escherichia coli* for secretory production of free haem. *Nat. Catal.* **1**, 720–728 (2018).
34. Monk, J. M. et al. iML1515, a knowledgebase that computes *Escherichia coli* traits. *Nat. Biotechnol.* **35**, 904–908 (2017).

Acknowledgements

This work was supported by the ‘Bio & Medical Technology Development Program (2021M3A9I4022740)’ of the National Research Foundation and funded by the Ministry of Science and ICT, Republic of Korea (K.R.C., Z.W.L., G.B.K., H.X. and S.Y.L.). This work was also supported by the ‘Cooperative Research Program for Agriculture

Science and Technology Development (Project No. RS-2021-RD009210)’ from the Rural Development Administration, Republic of Korea (K.R.C. and Z.W.L.).

Author contributions

K.R.C. and S.Y.L. conceptualized the project. K.R.C., Z.W.L. and G.B.K. developed the methodology. K.R.C., Z.W.L., G.B.K. and H.X. conducted experiments. K.R.C., Z.W.L., G.B.K. and H.X. analyzed the data. K.R.C., Z.W.L. and G.B.K. performed visualization. K.R.C., Z.W.L. and G.B.K. wrote the original draft. K.R.C. and S.Y.L. reviewed and edited the paper.

Competing interests

The authors declare no competing interests.

Additional information

Supplementary information The online version contains supplementary material available at <https://doi.org/10.1038/s44286-023-00022-0>.

Correspondence and requests for materials should be addressed to Sang Yup Lee.

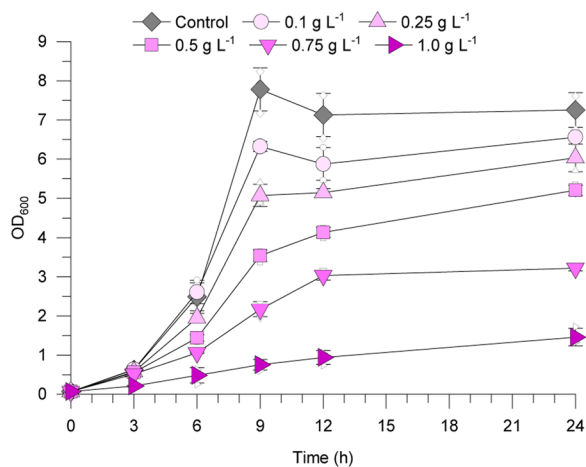
Peer review information *Nature Chemical Engineering* thanks Kristina Haslinger and the other, anonymous, reviewer(s) for their contribution to the peer review of this work.

Reprints and permissions information is available at www.nature.com/reprints.

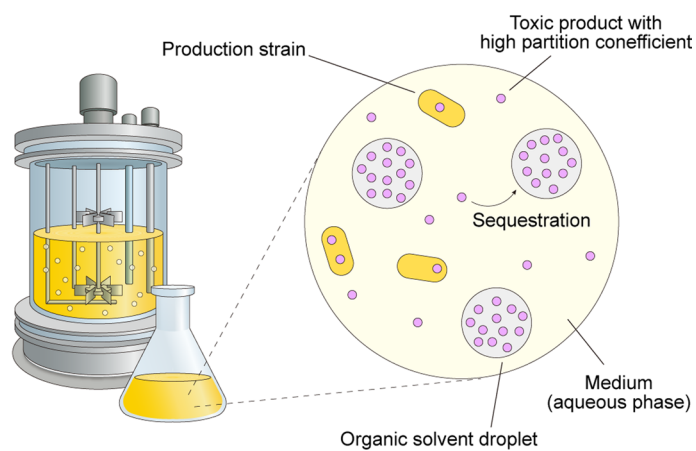
Publisher’s note Springer Nature remains neutral with regard to jurisdictional claims in published maps and institutional affiliations.

Springer Nature or its licensor (e.g. a society or other partner) holds exclusive rights to this article under a publishing agreement with the author(s) or other rightsholder(s); author self-archiving of the accepted manuscript version of this article is solely governed by the terms of such publishing agreement and applicable law.

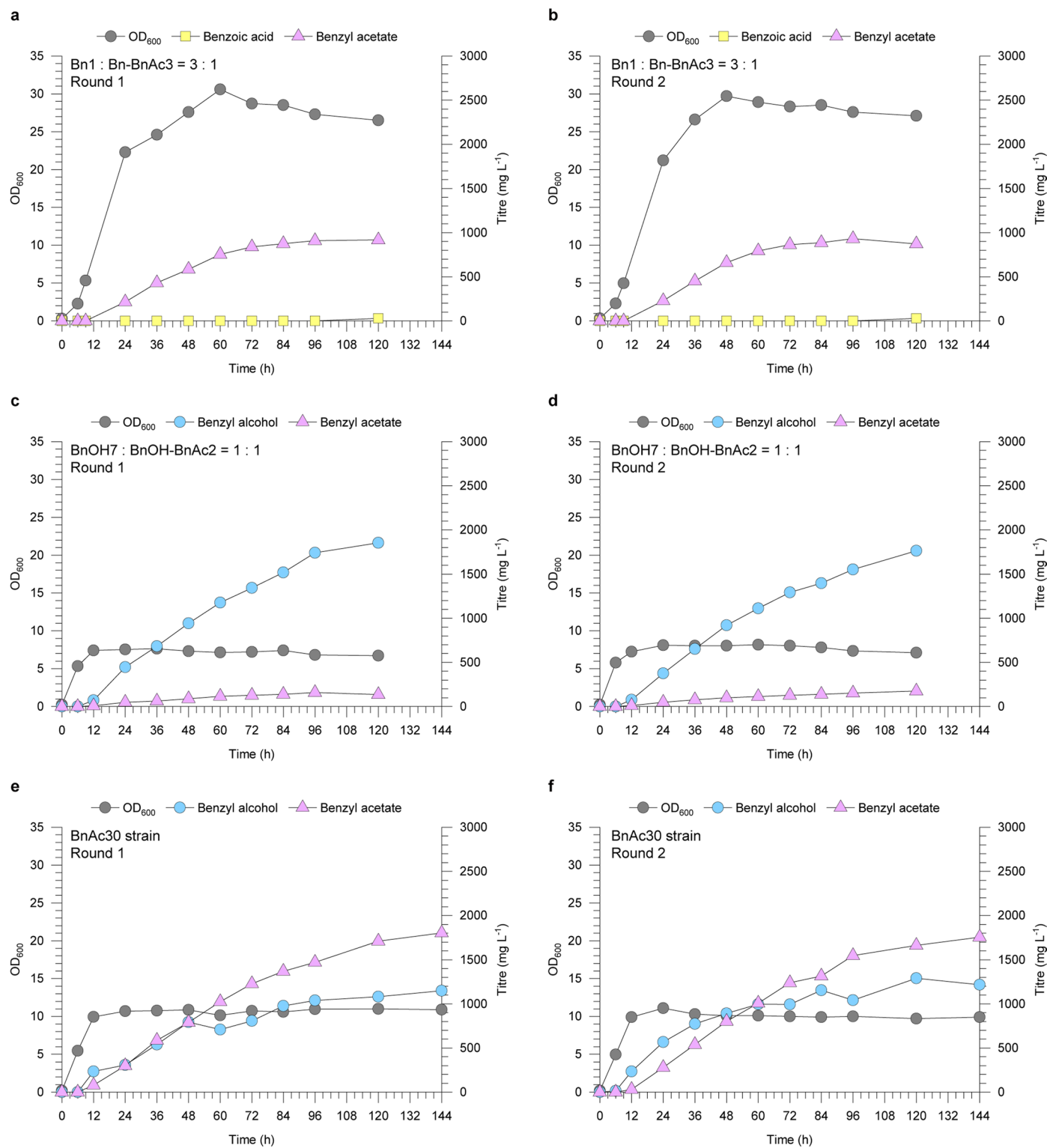
© The Author(s), under exclusive licence to Springer Nature America, Inc. 2024

a Benzyl acetate toxicity test

Extended Data Fig. 1 | Two-phase extractive fermentation to overcome benzyl acetate toxicity. **a**, The growth curve of *E. coli* W3110 strain in shake-flask culture supplemented with 0–1.0 g L⁻¹ of benzyl acetate. Solid symbols and error bars represent mean values and standard deviations of biological triplicates ($n = 3$). Smaller open symbols represent raw data points. **b**, Scheme of aqueous/

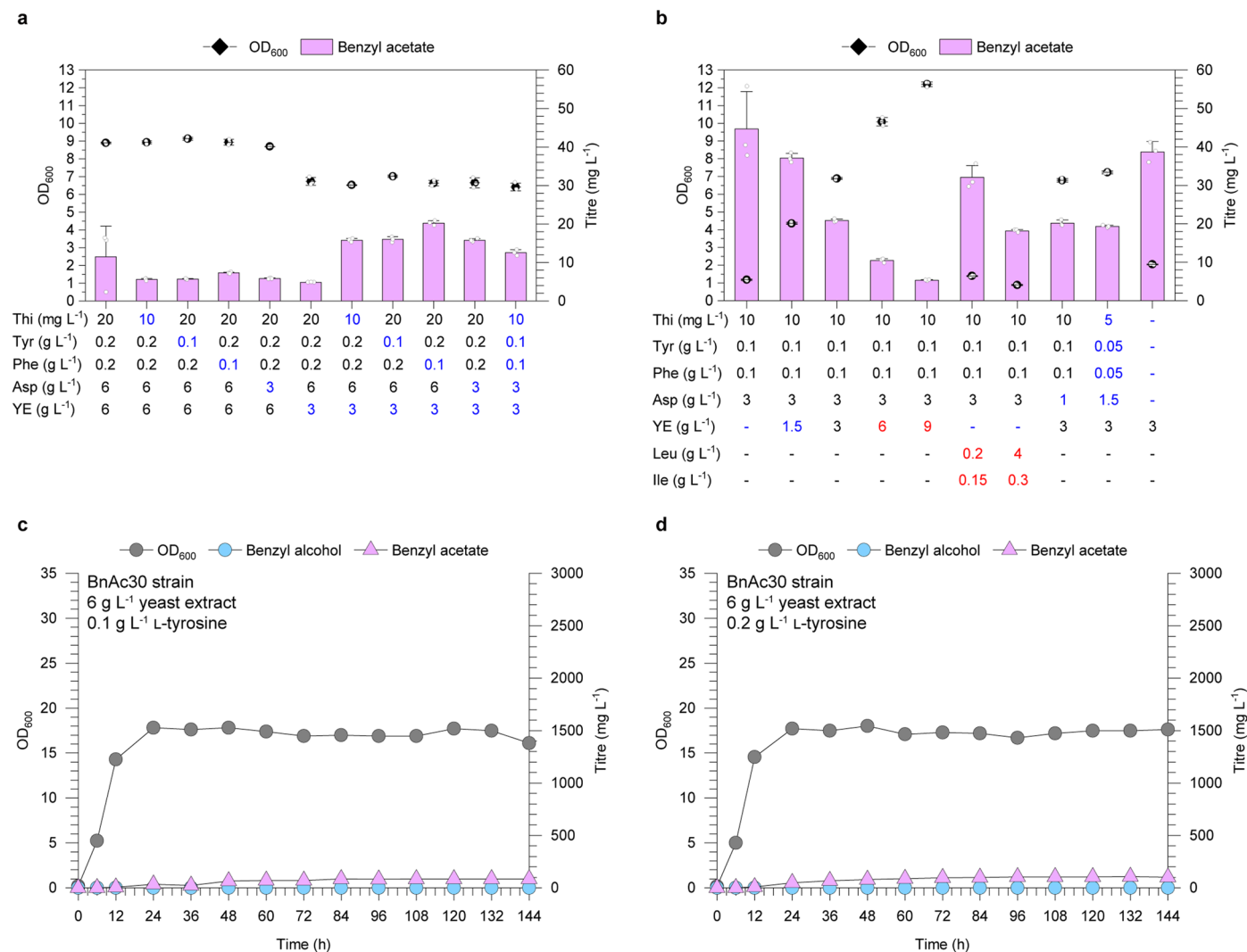
b Two-phase extractive culture

organic two-phase extractive culture. Toxic products with high hydrophobicity and partition coefficient, such as benzyl acetate, can be effectively sequestered to droplets of organic solvents. As a result, the concentration of the toxic compounds in the aqueous phase and the cytoplasm decreases, leading to reduction of the toxic effects on microorganisms in the aqueous phase.



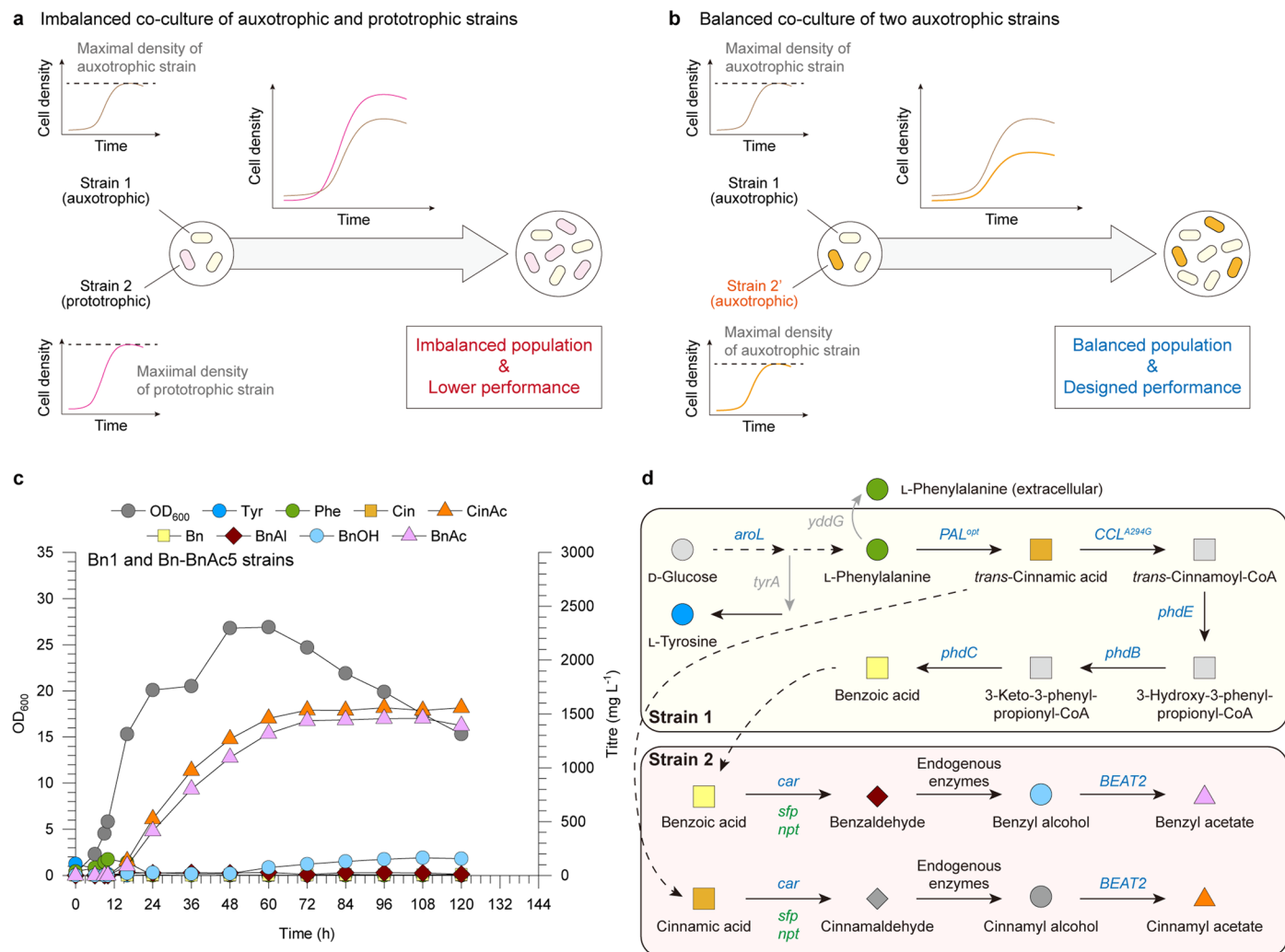
Extended Data Fig. 2 | Non-averaged profiles of two-phase extractive fermentations. **a** and **b**, Non-averaged profiles of the two-phase extractive fermentation for production of benzyl acetate by the co-culture of the Bn1 and Bn-BnAc3 strains. The averaged profile of these duplicated rounds of fermentations is presented in Fig. 2e. **c** and **d**, Non-averaged profiles of the two-phase extractive fermentation for production of benzyl acetate by the co-culture

of the BnOH7 and BnOH-BnAc2 strains. The averaged profile of these duplicated rounds of fermentation is presented in Fig. 3d. **e** and **f**, Non-averaged profiles of the two-phase extractive fermentation for production of benzyl acetate by the BnAc30 strain. The averaged profile of these duplicated rounds of fermentations are presented in Fig. 4e.



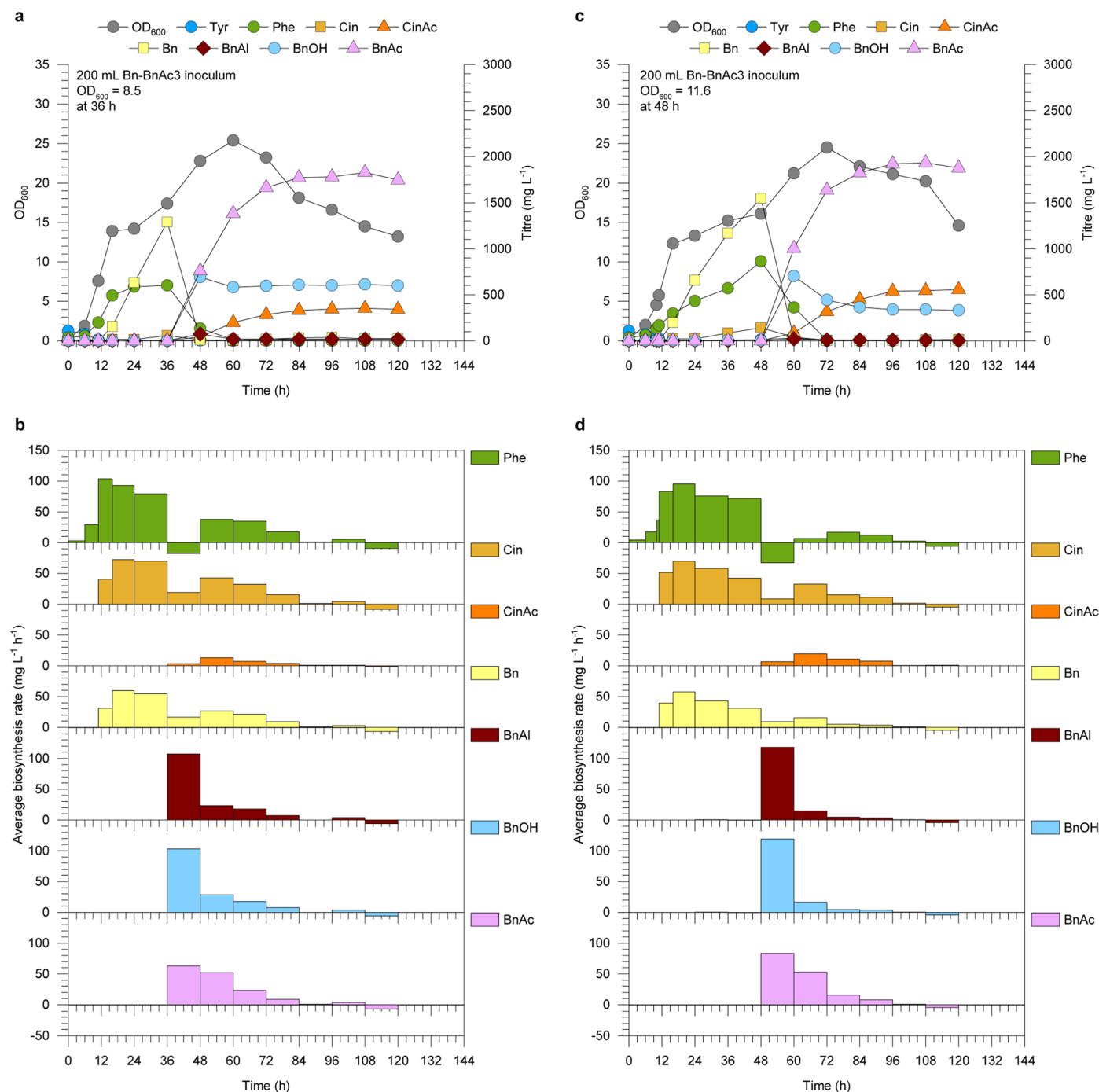
Extended Data Fig. 3 | Optimization of medium components to improve the cell density and benzyl acetate titre of the BnAc30 strain. **a**, Perturbation of component levels in shake-flask culture of the BnAc30 strain supplemented with increased amount of D-glucose (20 g L⁻¹), thiamine (Thi), L-tyrosine (Tyr), L-phenylalanine (Phe), L-aspartic acid (Asp) and yeast extract (YE) than the standard conditions. Bars and solid symbols represent mean values and error bars represent standard deviations of biological triplicates ($n = 3$). Smaller open symbols represent raw data points. **b**, Perturbation of component levels in shake-flask culture of the BnAc30 strain supplemented with 20 g L⁻¹ of D-glucose,

as well as replacement of yeast extract with L-leucine (Leu) and L-isoleucine (Ile). Bars and solid symbols represent mean values and error bars represent standard deviations of biological triplicates ($n = 3$). Smaller open symbols represent raw data points. **c**, Two-phase extractive fermentation of the BnAc30 strain with supplementation of 6 g L⁻¹ of yeast extract and 0.1 g L⁻¹ of L-tyrosine. Symbols represent raw data points ($n = 1$). **d**, Two-phase extractive fermentation of the BnAc30 strain with supplementation of 6 g L⁻¹ of yeast extract and 0.2 g L⁻¹ of L-tyrosine. Symbols represent raw data points ($n = 1$).



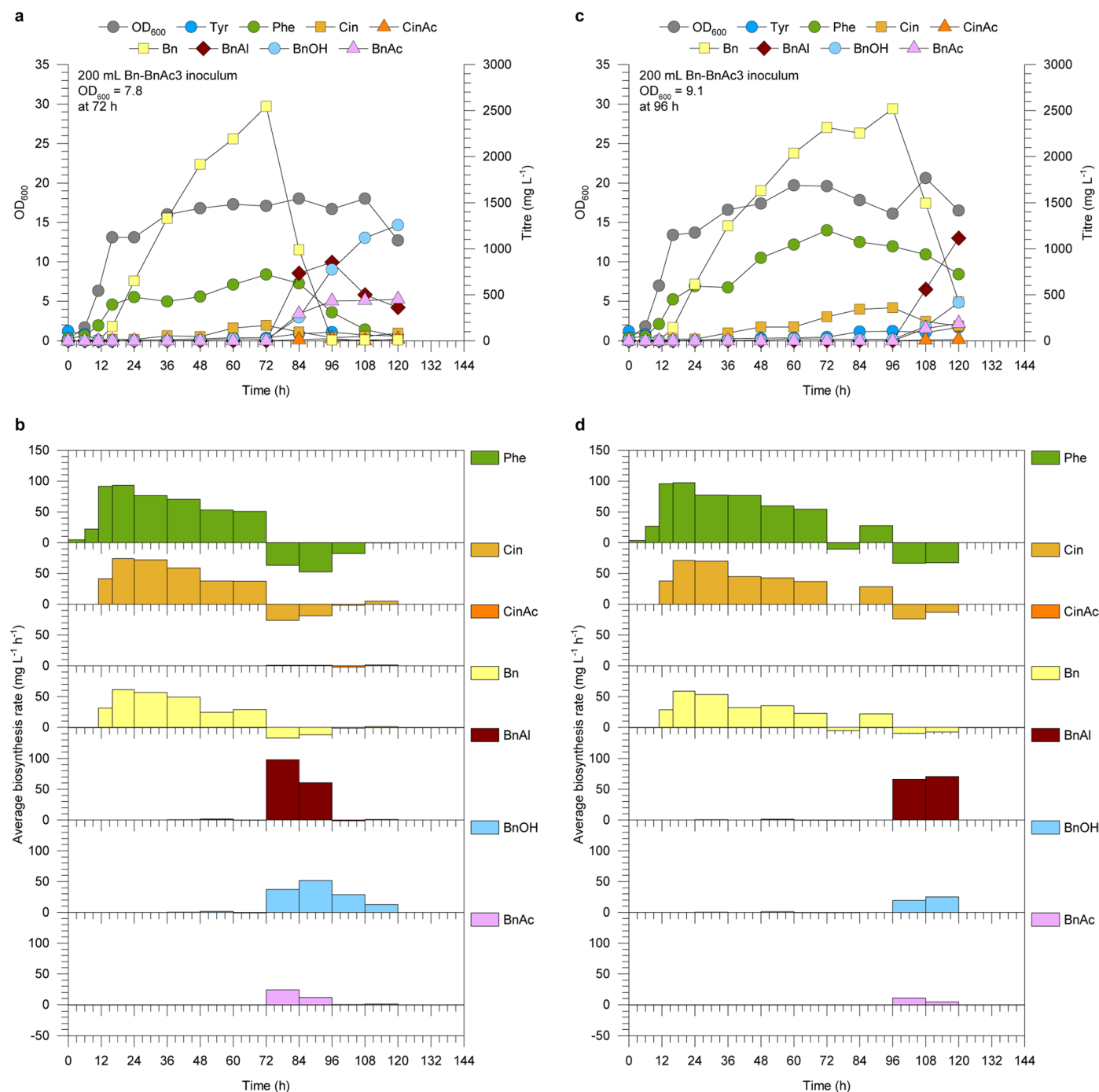
Extended Data Fig. 4 | Co-culture of the auxotrophic Bn-BnAc5 strain with the auxotrophic Bn1 strain. **a**, Population changes in co-culture of an auxotrophic upstream strain (strain 1) and a prototrophic downstream strain (strain 2). **b**, Population changes in co-culture of an auxotrophic upstream strain (strain 1) and an auxotrophic downstream strain (strain 2). **c**, Two-phase extractive fermentation profile for benzyl acetate production by co-culture of the

auxotrophic Bn1 strain and the auxotrophic Bn-BnAc5 strain. Symbols represent raw data points ($n = 1$). **d**, Scheme of promiscuous conversion of *trans*-cinnamic acid into cinnamyl acetate in co-culture of an upstream strain (strain 1) and a downstream strain (strain 2) harbouring the benzoic acid-dependent pathway for benzyl acetate production.



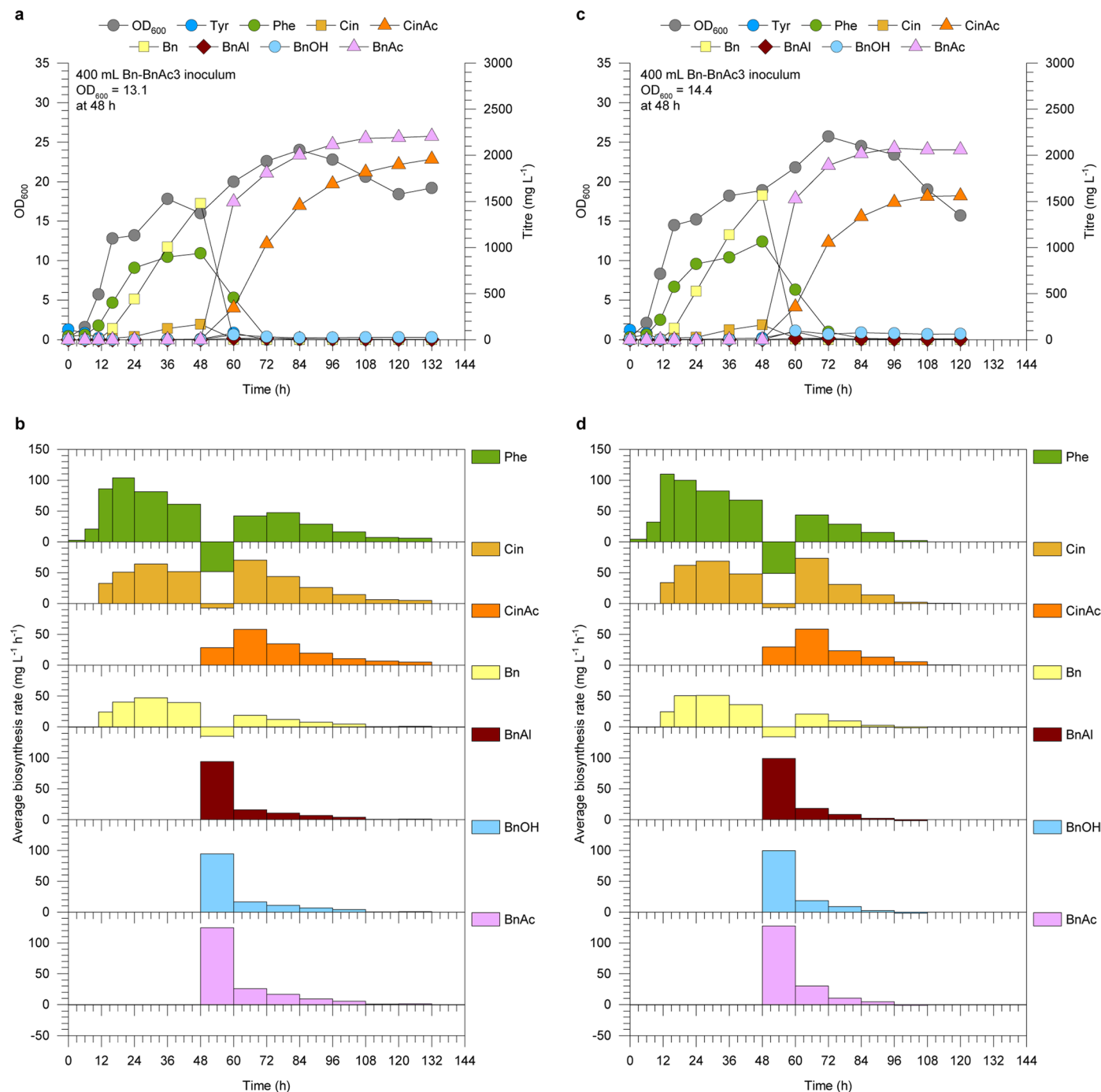
Extended Data Fig. 5 | Optimization of inoculation delay in delayed co-culture of the Bn1 and Bn-BnAc3 strains (part 1). **a**, Two-phase extractive fermentation profile of delayed co-culture of the Bn1 and Bn-BnAc3 strains ($n = 1$). The Bn-BnAc3 strain inoculum (200 mL; OD₆₀₀ = 8.5) was added after 36 h of fermentation. **b**, Apparent average biosynthesis rates of L-phenylalanine (Phe), *trans*-cinnamic acid (Cin), cinnamyl acetate (CinAc), benzoic acid (Bn), benzaldehyde (BnAl), benzyl alcohol (BnOH) and benzyl acetate (BnAc), calculated based on the changes in titres (panel a) and the molar masses of

the compounds. **c**, Two-phase extractive fermentation profile of delayed co-culture of the Bn1 and Bn-BnAc3 strains ($n = 1$). The Bn-BnAc3 strain inoculum (200 mL; OD₆₀₀ = 11.6) was added after 48 h of fermentation. **d**, Apparent average biosynthesis rates of benzyl acetate, cinnamyl acetate and intermediates between sampling points were calculated based on the changes in the titres (panel c) and the molar masses of the compounds. Symbols represent raw data points and bars represent apparent average biosynthesis rates.



Extended Data Fig. 6 | Optimization of inoculation delay in delayed co-culture of the Bn1 and Bn-BnAc3 strains (part 2). **a**, Two-phase extractive fermentation profile of delayed co-culture of the Bn1 and Bn-BnAc3 strains ($n = 1$). The Bn-BnAc3 strain inoculum (200 mL; OD₆₀₀ = 7.8) was added after 72 h of fermentation. **b**, Apparent average biosynthesis rates of L-phenylalanine (Phe), *trans*-cinnamic acid (Cin), cinnamyl acetate (CinAc), benzoic acid (Bn), benzaldehyde (BnAl), benzyl alcohol (BnOH) and benzyl acetate (BnAc), calculated based on the changes in titres (panel a) and the molar masses of

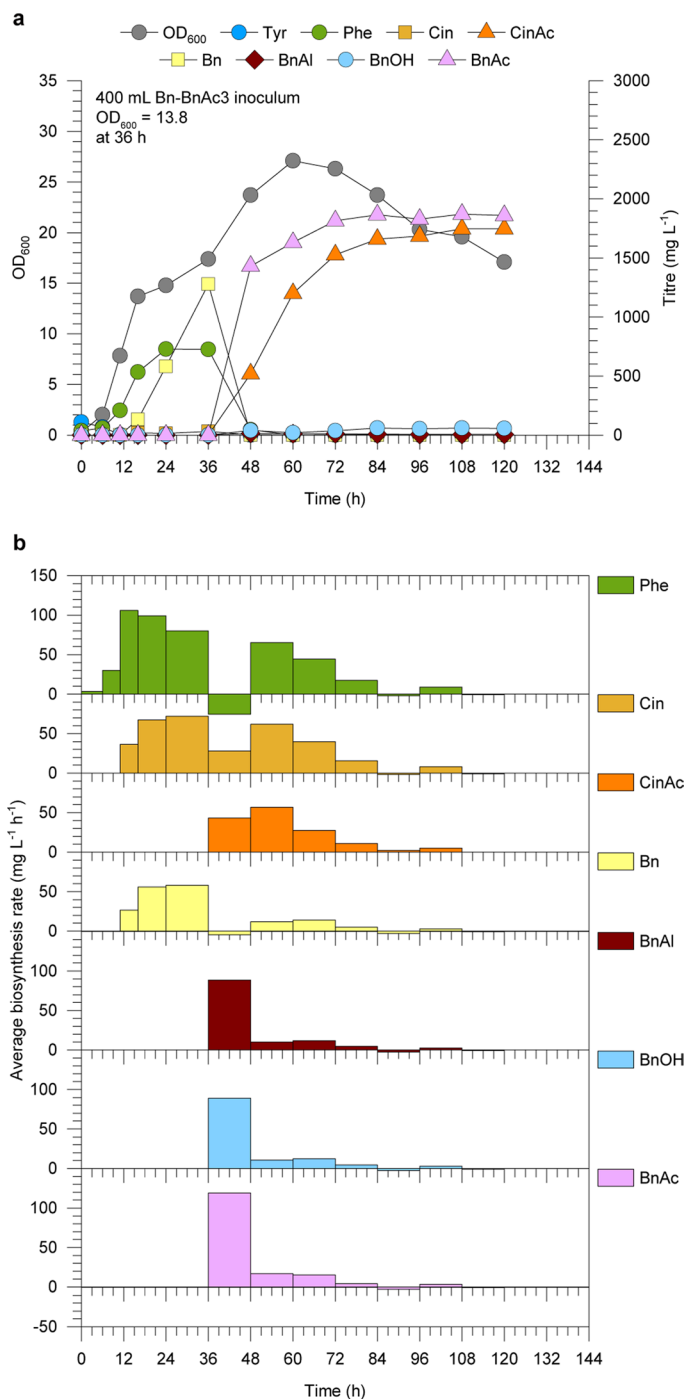
the compounds. **c**, Two-phase extractive fermentation profile of delayed co-culture of the Bn1 and Bn-BnAc3 strains ($n = 1$). The Bn-BnAc3 strain inoculum (200 mL; OD₆₀₀ = 9.1) was added after 96 h of fermentation. **d**, Apparent average biosynthesis rates of benzyl acetate, cinnamyl acetate and intermediates between sampling points were calculated based on the changes in the titres (panel c) and the molar masses of the compounds. Symbols represent raw data points and bars represent apparent average biosynthesis rates.



Extended Data Fig. 7 | Non-averaged profiles and average biosynthesis rates for the delayed co-culture of the Bn1 and Bn-BnAc3 strains shown in Fig. 5d.

a, Non-averaged two-phase extractive fermentation profile of delayed co-culture of the Bn1 and Bn-BnAc3 strains ($n = 1$). The Bn-BnAc3 strain inoculum (400 mL; OD₆₀₀ = 13.1) was added after 48 h of fermentation. The profiles of D-glucose and organic acids are summarized in Extended Data Fig. 10a. **b**, Apparent average biosynthesis rates of L-phenylalanine (Phe), *trans*-cinnamic acid (Cin), cinnamyl acetate (CinAc), benzoic acid (Bn), benzaldehyde (BnAl), benzyl alcohol (BnOH) and benzyl acetate (BnAc), calculated based on the changes in titres (panel a)

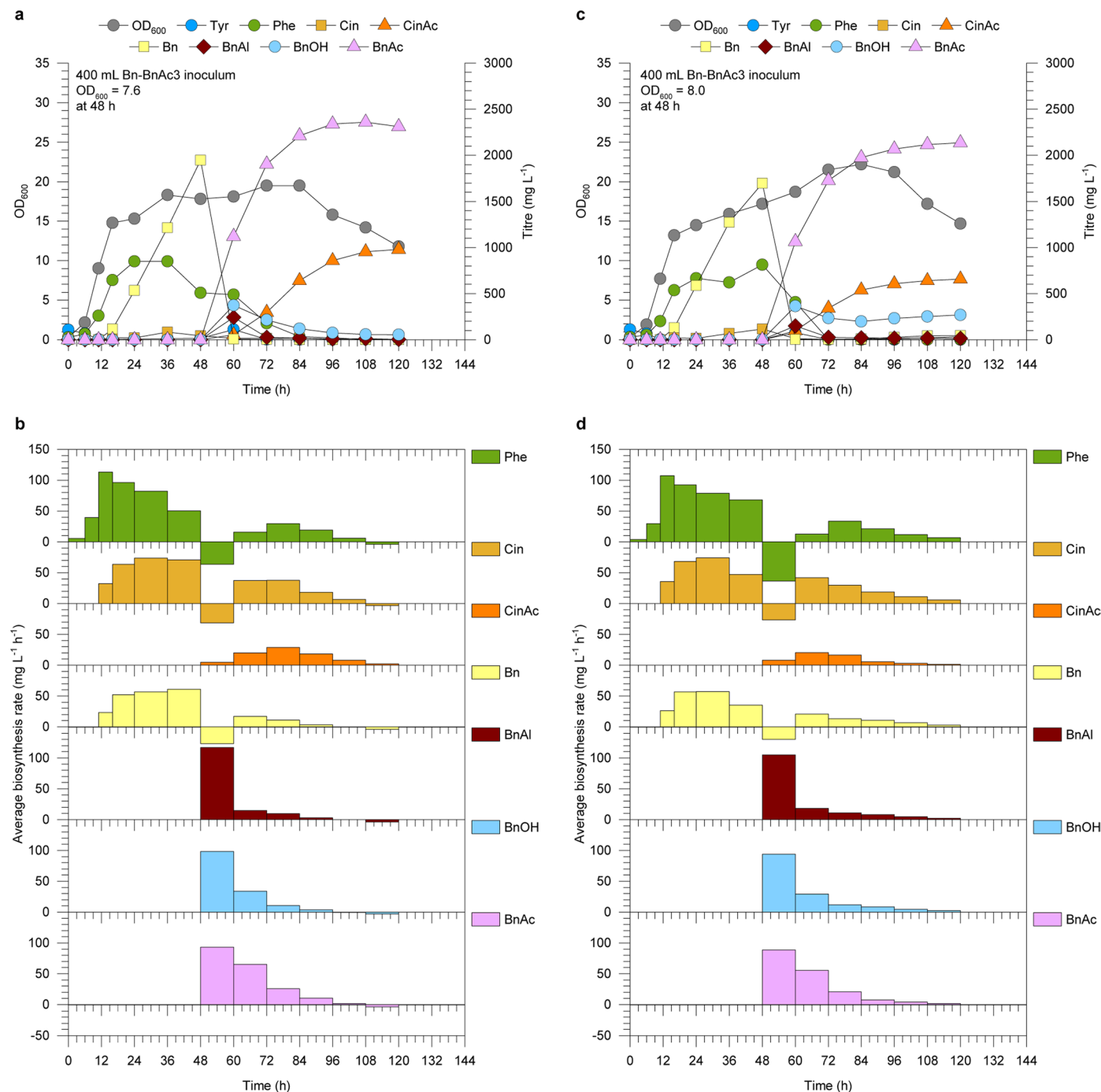
and the molar masses of the compounds. **c**, Non-averaged two-phase extractive fermentation profile of delayed co-culture of the Bn1 and Bn-BnAc3 strains ($n = 1$). The Bn-BnAc3 strain inoculum (400 mL; OD₆₀₀ = 14.4) was added after 48 h of fermentation. The profiles of D-glucose and organic acids are summarized in Extended Data Fig. 10b. **d**, Apparent average biosynthesis rates of benzyl acetate, cinnamyl acetate and intermediates between sampling points were calculated based on the changes in the titres (panel c) and the molar masses of the compounds. Symbols represent raw data points and bars represent apparent average biosynthesis rates.



Extended Data Fig. 8 | Two-phase extractive fermentation profile and average biosynthesis rates for the delayed co-culture of the Bn1 and Bn-BnAc3 strains with the delayed inoculum volume of 400 mL and inoculation delay of 36 h.

a, Two-phase extractive fermentation profile of delayed co-culture of the Bn1 and Bn-BnAc3 strains ($n = 1$). The Bn-BnAc3 strain inoculum (400 mL; $OD_{600} = 13.8$) was added after 36 h of fermentation. **b**, Apparent average biosynthesis rates

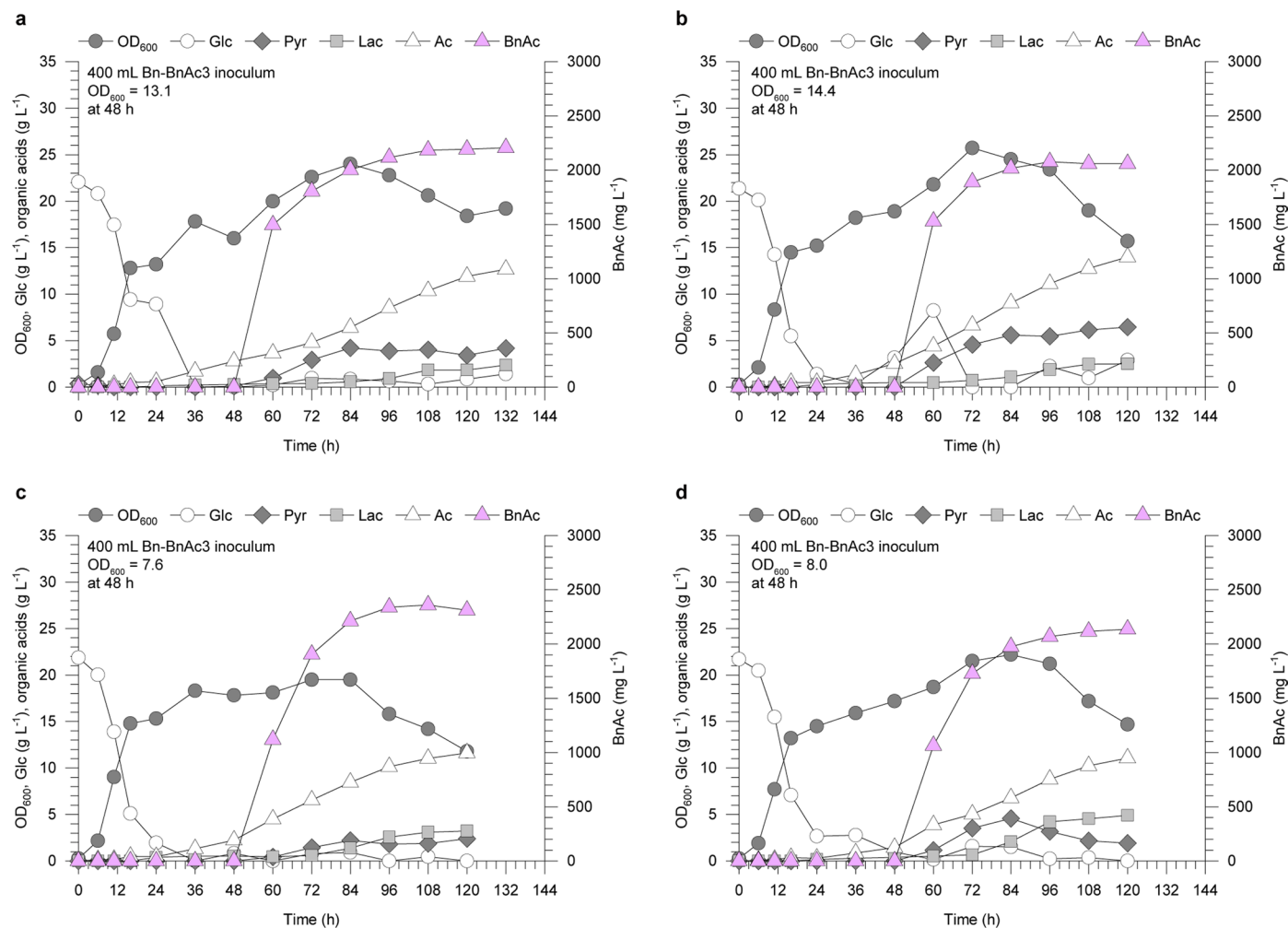
of L-phenylalanine (Phe), *trans*-cinnamic acid (Cin), cinnamyl acetate (CinAc), benzoic acid (Bn), benzaldehyde (BnAl), benzyl alcohol (BnOH) and benzyl acetate (BnAc), calculated based on the changes in titres (panel a) and the molar masses of the compounds. Symbols represent raw data points and bars represent apparent average biosynthesis rates.



Extended Data Fig. 9 | Non-averaged profiles and average biosynthesis rates for the delayed co-culture of the Bn1 and Bn-BnAc3 strains shown in Fig. 5e.

a, Non-averaged two-phase extractive fermentation profile of delayed co-culture of the Bn1 and Bn-BnAc3 strains ($n = 1$). The Bn-BnAc3 strain inoculum (400 mL; OD₆₀₀ = 7.6) was added after 48 h of fermentation. The profiles of D-glucose and organic acids are summarized in Extended Data Fig. 10c. **b**, Apparent average biosynthesis rates of L-phenylalanine (Phe), *trans*-cinnamic acid (Cin), cinnamyl acetate (CinAc), benzoic acid (Bn), benzaldehyde (BnAl), benzyl alcohol (BnOH) and benzyl acetate (BnAc), calculated based on the changes in titres (panel a)

and the molar masses of the compounds. **c**, Non-averaged two-phase extractive fermentation profile of delayed co-culture of the Bn1 and Bn-BnAc3 strains ($n = 1$). The Bn-BnAc3 strain inoculum (400 mL; OD₆₀₀ = 8.0) was added after 48 h of fermentation. The profiles of D-glucose and organic acids are summarized in Extended Data Fig. 10d. **d**, Apparent average biosynthesis rates of benzyl acetate, cinnamyl acetate and intermediates between sampling points were calculated based on the changes in the titres (panel c) and the molar masses of the compounds. Symbols represent raw data points and bars represent apparent average biosynthesis rates.



Extended Data Fig. 10 | Non-averaged D-glucose and organic acid profiles for the delayed co-culture of the Bn1 and Bn-BnAc3 strains shown in Extended Data Figs. 7 and 9. **a**, Non-averaged D-glucose and organic acid profiles during the delayed co-culture of the Bn1 and Bn-BnAc3 strains ($n = 1$) shown in Extended Data Fig. 7a. The Bn-BnAc3 strain inoculum (400 mL; $OD_{600} = 13.1$) was added after 48 h of fermentation. **b**, Non-averaged D-glucose and organic acid profiles for the delayed co-culture of the Bn1 and Bn-BnAc3 strains ($n = 1$) shown in Extended Data Fig. 7c. The Bn-BnAc3 strain inoculum (400 mL; $OD_{600} = 14.4$) was

added after 48 h of fermentation. **c**, Non-averaged D-glucose and organic acid profiles for the delayed co-culture of the Bn1 and Bn-BnAc3 strains ($n = 1$) shown in Extended Data Fig. 9a. The Bn-BnAc3 strain inoculum (400 mL; $OD_{600} = 7.6$) was added after 48 h of fermentation. **d**, Non-averaged D-glucose and organic acid profiles for the delayed co-culture of the Bn1 and Bn-BnAc3 strains ($n = 1$) shown in Extended Data Fig. 9c. The Bn-BnAc3 strain inoculum (400 mL; $OD_{600} = 8.0$) was added after 48 h of fermentation.

Reporting Summary

Nature Portfolio wishes to improve the reproducibility of the work that we publish. This form provides structure for consistency and transparency in reporting. For further information on Nature Portfolio policies, see our [Editorial Policies](#) and the [Editorial Policy Checklist](#).

Statistics

For all statistical analyses, confirm that the following items are present in the figure legend, table legend, main text, or Methods section.

- | n/a | Confirmed |
|-------------------------------------|--|
| <input type="checkbox"/> | <input checked="" type="checkbox"/> The exact sample size (n) for each experimental group/condition, given as a discrete number and unit of measurement |
| <input checked="" type="checkbox"/> | <input type="checkbox"/> A statement on whether measurements were taken from distinct samples or whether the same sample was measured repeatedly |
| <input checked="" type="checkbox"/> | <input type="checkbox"/> The statistical test(s) used AND whether they are one- or two-sided
<i>Only common tests should be described solely by name; describe more complex techniques in the Methods section.</i> |
| <input checked="" type="checkbox"/> | <input type="checkbox"/> A description of all covariates tested |
| <input checked="" type="checkbox"/> | <input type="checkbox"/> A description of any assumptions or corrections, such as tests of normality and adjustment for multiple comparisons |
| <input type="checkbox"/> | <input checked="" type="checkbox"/> A full description of the statistical parameters including central tendency (e.g. means) or other basic estimates (e.g. regression coefficient) AND variation (e.g. standard deviation) or associated estimates of uncertainty (e.g. confidence intervals) |
| <input checked="" type="checkbox"/> | <input type="checkbox"/> For null hypothesis testing, the test statistic (e.g. F , t , r) with confidence intervals, effect sizes, degrees of freedom and P value noted
<i>Give P values as exact values whenever suitable.</i> |
| <input checked="" type="checkbox"/> | <input type="checkbox"/> For Bayesian analysis, information on the choice of priors and Markov chain Monte Carlo settings |
| <input checked="" type="checkbox"/> | <input type="checkbox"/> For hierarchical and complex designs, identification of the appropriate level for tests and full reporting of outcomes |
| <input checked="" type="checkbox"/> | <input type="checkbox"/> Estimates of effect sizes (e.g. Cohen's d , Pearson's r), indicating how they were calculated |

Our web collection on [statistics for biologists](#) contains articles on many of the points above.

Software and code

Policy information about [availability of computer code](#)

Data collection OpenLAB CDS (ChemStation Edition; version information unavailable) and Breeze2 (Database version 6.20.00.00) were used for analyzing metabolite concentrations in shake-flask and fed-batch fermentation samples.

Data analysis Custom codes used for metabolic flux analysis and techno-economic analysis (based on BioSTEAM platform; version information unavailable) are available at <https://github.com/kaistsystemsbiology/BenzylAcetateFluxAnalysis> and <https://github.com/kaistsystemsbiology/BenzylAcetateTEA>.

For manuscripts utilizing custom algorithms or software that are central to the research but not yet described in published literature, software must be made available to editors and reviewers. We strongly encourage code deposition in a community repository (e.g. GitHub). See the Nature Portfolio [guidelines for submitting code & software](#) for further information.

Data

Policy information about [availability of data](#)

All manuscripts must include a [data availability statement](#). This statement should provide the following information, where applicable:

- Accession codes, unique identifiers, or web links for publicly available datasets
- A description of any restrictions on data availability
- For clinical datasets or third party data, please ensure that the statement adheres to our [policy](#)

All source data for the (extended data) figures were deposited in Figshare (<https://doi.org/10.6084/m9.figshare.24026634>).

The catalytic information of the enzymatic reactions involved in converting benzoic acid into benzaldehyde (EC 1.2.1.30) and benzyl alcohol/acetyl-CoA into benzyl acetate (EC 2.3.1.224 and EC 2.3.1.84) can be searched from the in the online enzyme database BRENDA (<https://www.brenda-enzymes.org>).

Research involving human participants, their data, or biological material

Policy information about studies with [human participants or human data](#). See also policy information about [sex, gender \(identity/presentation\), and sexual orientation](#) and [race, ethnicity and racism](#).

Reporting on sex and gender	<input type="text" value="Not applicable to this study"/>
Reporting on race, ethnicity, or other socially relevant groupings	<input type="text" value="Not applicable to this study"/>
Population characteristics	<input type="text" value="Not applicable to this study"/>
Recruitment	<input type="text" value="Not applicable to this study"/>
Ethics oversight	<input type="text" value="Not applicable to this study"/>

Note that full information on the approval of the study protocol must also be provided in the manuscript.

Field-specific reporting

Please select the one below that is the best fit for your research. If you are not sure, read the appropriate sections before making your selection.

Life sciences Behavioural & social sciences Ecological, evolutionary & environmental sciences

For a reference copy of the document with all sections, see [nature.com/documents/nr-reporting-summary-flat.pdf](https://www.nature.com/documents/nr-reporting-summary-flat.pdf)

Life sciences study design

All studies must disclose on these points even when the disclosure is negative.

Sample size	<input type="text" value="Shake-flask culture were conducted in triplicate, a widely used sample size to evaluate the performance of microbial strains at the flask level. Fermentations were conducted in duplicates due to limitation of the availability."/>
Data exclusions	<input type="text" value="No data were excluded from the analyses."/>
Replication	<input type="text" value="Shake-flask culture results were reproducible in triplicated rounds of experiments. Fermentation results also showed consistency in duplicated rounds of experiments. Other experiments, including simulations, also showed consistent results for more than duplicated rounds of experiments."/>
Randomization	<input type="text" value="Single colonies for experiments were randomly selected from plates among tens to thousands of colonies with similar appearance."/>
Blinding	<input type="text" value="The investigators were blinded to the group allocation during flask culture by assigning temporary identifiers to the samples during experiments."/>

Reporting for specific materials, systems and methods

We require information from authors about some types of materials, experimental systems and methods used in many studies. Here, indicate whether each material, system or method listed is relevant to your study. If you are not sure if a list item applies to your research, read the appropriate section before selecting a response.

Materials & experimental systems

n/a	Involved in the study
<input checked="" type="checkbox"/>	<input type="checkbox"/> Antibodies
<input checked="" type="checkbox"/>	<input type="checkbox"/> Eukaryotic cell lines
<input checked="" type="checkbox"/>	<input type="checkbox"/> Palaeontology and archaeology
<input checked="" type="checkbox"/>	<input type="checkbox"/> Animals and other organisms
<input checked="" type="checkbox"/>	<input type="checkbox"/> Clinical data
<input checked="" type="checkbox"/>	<input type="checkbox"/> Dual use research of concern
<input checked="" type="checkbox"/>	<input type="checkbox"/> Plants

Methods

n/a	Involved in the study
<input checked="" type="checkbox"/>	<input type="checkbox"/> ChIP-seq
<input checked="" type="checkbox"/>	<input type="checkbox"/> Flow cytometry
<input checked="" type="checkbox"/>	<input type="checkbox"/> MRI-based neuroimaging